*Annu. Rev. Astron. Astrophys. 1992. 30: 75–112*


# ASTRONOMICAL MASERS

*Moshe Elitzur*

Department of Physics and Astronomy, University of Kentucky, Lexington, Kentucky 40506 and NASA Ames Research Center, MS 245-3, Moffett Field, California 94035

KEY WORDS: late-type stars, star-forming regions, shock waves, interstellar molecules, magnetic fields

## 1. INTRODUCTION

Astronomical masers were discovered more than 25 years ago. They were first reviewed in this series by Litvak (1974), and again by Reid & Moran (1981). In the ten years since the last review, research activity in this area has experienced an explosive growth, thanks mostly to continuing progress in interferometric techniques. The expected completion of the VLBA and the prospects for space VLBI ensure that the field will continue to expand at an accelerated pace for many years.

This review attempts to cover the main developments since the last review by Reid & Moran. The large volume of research activity makes it likely that this could be the last time a comprehensive coverage of the entire field is attempted in a single review. It is likely that future reviews will be limited to subsets of this field, broken perhaps along the lines chosen here for organization of the material. The first two sections are devoted to phenomenology—observations and modeling of Galactic (Section 2) and extragalactic (Section 3) maser sources. Section 4 describes developments concerning the physical properties of maser radiation, those special characteristics that set it apart from thermal radiation. Finally, Section 5 covers a new and exciting trend: the use of masers as general tools for study of the astronomical environments where the radiation is produced and in which it propagates.

## 2. PHENOMENOLOGY—GALACTIC MASERS

Recently, several new types of masers have been discovered. Separate sections are devoted below to studies of new sub-mm $H_2O$, $CH_3OH$, and $NH_3$ masers. Maser emission from HCN was discovered by Guilloteau et



0066–4146/92/0915–0075$02.00

al (1987) in the carbon-rich late-type star CIT 6. This maser action bears some resemblance to SiO, as it occurs in the $J = 1 \rightarrow 0$ rotation line in an excited vibration state. Strong maser emission in the $J = 2 \rightarrow 1$ transition of another vibration state was subsequently detected in IRC 10216 by Lucas & Cernicharo (1989). A new class of unusual circumstellar masers was identified by Likkel & Morris (1988) and te Lintel Hekkert et al (1988). It includes evolved stars characterized by OH and $H_2O$ maser emission distributed over an exceedingly large velocity range of 100–300 km $s^{-1}$. Detailed observations by Likkel et al (1991) led them to propose a bipolar geometry, with an equatorial disk involved in the collimation of a high velocity wind streaming along the polar axis. Another new type of maser was discovered in hydrogen radio recombination lines in the emission line source MWC 349. Martin-Pintado et al (1989a) found dramatic changes in several characteristics of the Hn$\alpha$ recombination line emission around 1 mm (n = 31): The profile changes from Gaussian to double-peak shape and the intensity increases appreciably, rising with line frequency. The proposal that this behavior reflects maser emission was supported by subsequent detection of time variability for these lines, the first for radio recombination lines (Martin-Pintado et al 1989b). A two-year monitoring project by Gordon (1991) confirmed the variability and showed that the velocity separation and intensity ratio of the two peaks vary in a similar way to variations often seen in Be stars. Level calculations by Walmsley (1990) identified the range of physical parameters where these transitions can be inverted. These results were used by Ponomarev et al (1990) for modeling.

The main ingredient fueling advances in maser research continues to be the constant progress in interferometric techniques, progress that enables better understanding of the maser process as well as the overall structure and kinematics of the sources. For example, Chapman & Cohen (1986) reconstructed the velocity field around VX Sgr by combining maps of its SiO, $H_2O$, and OH masers. The combined map provides conclusive evidence for the wind acceleration and the shell structure of the various maser species. Most of the studies described below have similarly benefited from progress in spatial resolution.

## 2.1 *OH*

2.1.1 LATE-TYPE STARS High frequency-resolution 1612 MHz spectra of supergiants by Cohen et al (1987) indicate that circular polarization, which revealed itself in sharp reversals in the profile of the parameter $V$, may be common in these sources. Inferred field strengths are $\sim 1$ mG. Together with SiO polarization measurements (Section 2.3.1), a variation of field strength with distance from the star of $\sim r^{-2}$–$r^{-3}$ can be deduced. Similar

observations by Zell & Fix (1991) reveal considerably smaller fields in OH/IR stars.

Interferometric mapping of the type II OH/IR star OH127.8 by Booth et al (1981) provided strong and direct confirmation of the "front-back" explanation for the 1612 MHz double-peak profile. Additional support comes from phase-lag measurements, greatly expanded by Herman & Habing (1985b). These measurements determine the radius of the OH shell, with values from just under $\sim 10^{16}$ cm all the way to $\gtrsim 10^{17}$ cm, providing one of only a handful of methods in astronomy that actually measure a linear dimension. In addition, high-resolution interferometry can be used to determine the shell's angular size. Assuming spherical symmetry (an excellent overall assumption in general), the two measurements combined yield the distance to the source. This method was used very effectively by Herman & Habing (1985a,b) to determine distances to OH/IR stars. They point out that distance measurements to external galaxies may also be possible.

Early confirmations of far-IR pumping for the 1612 MHz masers were followed by more detailed work. Dickinson (1987) compared the ratio of the number of photons in the maser and IR bands in various subgroups of OH/IR stars and concluded that the intrinsic efficiencies of pumping by 35 $\mu$m and 53 $\mu$m are similar, in agreement with theoretical modeling. Cohen (1989) showed that far-IR pumping considerations constrain the masers to a triangular region in the $\log \dot{M} - \log r$ plane. Using data from Bowers (1985) he then showed that all the observations indeed fall in the allowed region. Dickinson (1991) finds that at low mass loss rates, $\dot{M} \lesssim 10^{-6}\, M_\odot\ \mathrm{yr}^{-1}$, the pumping efficiency increases with $\dot{M}$. This is the expected behavior for a radiative pump when the pump transitions are optically thin, since the absorption of pump photons increases with $\dot{M}$.

In spite of its success in explaining the observations, an ideal, radial flow obviously cannot always provide the full, correct description. Even in the case of OH127.8, the shell structure is rather clumpy and incomplete. This is typical. The effect of irregularities on maser emission was analyzed in an elegant manner by Deguchi (1982). Further work along similar lines was performed by Szymczak (1989, 1990), and more is called for.

Main-line maser emission did not generate as much research activity, and it can be hoped that this situation will change. These masers can provide important clues to the operation of megamaser galaxies (Section 3.1), as there are good indications that the pumping is similar in both sources.

2.1.2 HII/OH REGIONS; EXCITED STATE MASERS Much of the research in this area revolved around the nature of the masers' velocity field. The

proposal that the masers are located in the compressed shell between the shock and ionization fronts around the HII region (Elitzur & de Jong 1978) implies expansion. However, Reid et al (1980) observed that the centroid velocity of maser features in W3(OH) corresponds to a large redshift from the velocity of the recombination lines, which is expected to indicate the actual velocity of the HII region. They proposed that the HII region is still accreting matter and that the masers are located in accertion blobs rather than an expanding shell. This was disputed by Norris & Booth (1981) who argued that some of the maser spots were not projected against the HII region and therefore could be located behind it, thus redshift need not necessarily imply infall. Berulis & Ershov (1983) then noticed that a systematic trend in the velocities of the Hn$\alpha$ recombination lines could actually be attributed to optical depth effects and that the removal of this effect brings the recombination-line velocities into good agreement with the maser centroid velocity. Although the essence of this mechanism was confirmed in observations by Welch & Marr (1987), they find that the observed linewidth differs considerably from the one obtained by Berulis & Ershov. Thus the simple spherical expansion model used in that analysis is not entirely adequate, a point also emphasized by Wilson et al (1987).

The controversy appears to have been finally settled by the proper-motion experiment of Bloemhof et al (1989), which clearly shows that the general maser motion is expansion. There is even some indication that the apparent center of divergence is roughly coincident with the center of the compact HII region. Similar results were obtained for Cepheus A by Migenes et al (1991). However, although the central issue is seemingly resolved, the exact nature of the velocity field and the overall structure of HII/OH regions are far from understood. The first hint of a problem is the ongoing difficulty of modeling the recombination lines in W3(OH). Further indications come from the work of Wood & Churchwell (1989) who noted that the total number of ultracompact HII regions they found in an incomplete sample of the Galactic plane is inconsistent with a lifetime of $<3 \times 10^4$ yr—the typical expansion time prescribed by the sensitivity of their observations. It is evident that some basic ingredients are still missing from our understanding of the structure and evolution of ultracompact HII regions; they are considerably more complex than the simple objects described by Spitzer (1978), which Elitzur & de Jong (1978) have employed in their modeling. Cometary structure (Van Buren et al 1990) may be important for some sources while a disk structure is clearly evident in the maser observations of others (Brebner et al 1987).

Although the pumping of main lines in HII/OH regions remains a problem, some encouraging developments did take place, coming from a

somewhat unexpected direction—the study of OH excited states. The detection of the main lines of $^2\Pi_{1/2}(J = 3/2)$ and $^2\Pi_{1/2}(J = 5/2)$ in W3(OH) (Wilson et al 1990) completed the detection of radio transitions in all rotation states below 510 K in this source. Some lines display absorption, others "quasi-thermal" emission and some display narrow maser features, which can be quite bright; interferometric mapping reveals $T_b \gtrsim 10^9$ K (Baudry et al 1988). No obvious pattern can be discerned and the occurrence of emission and absorption appears random. Cesaroni & Walmsley (1991) performed a detailed model calculation, taking into account the competing effects of radiative and collisional excitations, radiative trapping, and line overlaps. They find that a suitable combination of far-IR radiation field and line overlap can qualitatively reproduce almost all the features observed in W3(OH), including the ground-state masers. Given the complexity displayed by the observed patterns, this success is an impressive accomplishment.

The adaptation of these calculations to the ground-state main-line masers would require more work. First, the inversion involves competition, whose details have not yet been analyzed, between radiative and collisional rates. It is not exactly clear how the inversion is accomplished nor what are the general thermodynamic constraints imposed on the maser intensities it can produce. Second, since all the ingredients included in the calculations exist also in late-type stars, what causes the great disparity between the intensities and line ratios of main-line masers in two environments? If line overlap played a significant role in determining pump efficiencies, perhaps a key distinction between the two situations would be the widely different velocity fields (see also Section 4.2). Finally, the availability of IR radiation field with the properties required by the model calculations remains problematic. The studies of Cohen et al (1988) and Moore et al (1988) show that IR photon luminosities are adequate to pump the masers. In particular, the latter study finds a correlation between far-IR and 1665 MHz emission in a large sample of HII/OH sources. However, the observed IR radiation is due to cool dust, located at a much larger distance from the central star than the OH masers. Thus, although the IR luminosity exceeds the OH luminosity, it is radiated from a much larger region; the IR photon emission rate of the maser region itself could be smaller than the OH photon luminosity (Norris & Booth 1981). Also, the rotation temperature of the excited states requires warm dust with $T_d \sim 160$ K, while the IR observations only give indications of cool dust with $T_d \lesssim 50$ K. A possible resolution of this difficulty may be to invoke clumps (the maser spots) subjected to an IR field different from the one observed from outside the region.

In spite of these difficulties, the success of the Cesaroni & Walmsley

calculations is a most encouraging development which holds the promise for deciphering the ground-state HII/OH masers. It is therefore important to establish the actual degree of correlation that may or may not exist among ground- and excited-state masers. In addition, more observational studies of the excited-state masers in late-type stars, somewhat neglected in recent years, would be valuable. Since the pump mechanism for the ground-state masers in these sources is fairly well established, they may provide clues about possible correlations with the excited-state patterns. Studies of the detailed structure of the IR field are also important.

## 2.2 $H_2O$

2.2.1 LATE-TYPE STARS Detailed cross sections for neutral collisions finally became available (Green 1980) and were utilized by Cooke & Elitzur (1985) to model the $H_2O$ masers; modeling with the newer cross sections by Palma et al (1988) produces similar results. These calculations confirmed an earlier conclusion by Deguchi (1977) that the pump mechanism is rotational collisional excitations and added a number of predictions that were since tested in observations. A predicted correlation of $H_2O$ maser luminosity with mass-loss rate is confirmed by Bowers & Hagen (1984), Nyman et al (1986), and Engels et al (1986). Both the correlation trend and the scale of the luminosities are in agreement with the theoretical results. A similar correlation of maser region size with mass-loss rate was verified by Lane et al (1987), again with good quantitative agreement. A predicted variation of the inner radius of the maser region with $\dot{M}^{2/3}v^{-1}$ is supported by published maps of $H_2O$ masers, analyzed by Cohen (1987). Lewis & Engles (1991) find that the IR color dependence of the detectability of $H_2O$ masers is properly explained by the collisional excitation model results.

2.2.2 STAR-FORMING REGIONS Because $H_2O$ is nonparamagnetic, its Zeeman pattern cannot be resolved by interstellar magnetic fields and circular polarization is only produced at the level of $\sim 10^{-4}$ for a field strength of 1 mG. Various ingenious techniques have been devised to extract such polarization from data, and Fiebig & Gusten (1989) employed these methods with great success in a study of $H_2O$ maser clumps. Inferred magnetic field strengths are typically a few tens of mG. These are the strongest magnetic fields measured to date in interstellar regions, and they extend the previously derived correlation between field strength and gas density (Troland & Heiles 1986) over five more decades of density.

Strong outbursts, such as the one in Orion, could turn out to be common in sources with many maser features; Liljestrom et al (1989) list six possibly similar events that occurred in W49 between 1969 and 1985. Inter-

ferometric studies have continued to provide increasingly detailed information about spatial structures and velocity fields. A new standard was set by the latest study of W49 by Gwinn et al (1991); combining measurements of five epochs they were able to trace the motion of 105 maser features and study the velocity field in great detail. A fairly complete prescription for modeling attempts has emerged (Genzel 1986): The $H_2O$ masers are locally created and pumped by the interaction of highly supersonic mass outflow from a central young star with clumps or inhomogeneities in the surrounding cloud. The masers have filamentary shape, with the axis perpendicular to the direction of motion. Typical parameters for maser spots are: diameter $\sim 10^{13}$ cm, aspect ratio $\sim 10$, density $\sim 10^9$ $cm^{-3}$, and brightness temperature $\sim 10^{12}$ K.

A first attempt at incorporating some of these properties into a comprehensive model was made by Tarter & Welch (1986), whose scheme required extremely dense ($\sim 10^9$ $cm^{-3}$) clumps, further compressed by powerful shocks. Subsequent calculations of high-velocity ($\gtrsim$40–50 km $s^{-1}$) magnetic J-shocks in less dense regions (pre-shock densities $\sim 10^7$ $cm^{-3}$) showed that they develop a high density ($\sim 10^9$ $cm^{-3}$), high post-shock temperature ($\sim$400 K) plateau, rich in $H_2O$. The high temperature is maintained by the reformation of $H_2$ molecules, following their initial dissociation, on grain surfaces and their subsequent ejection into the gas phase. This plateau suggests itself as a natural site for $H_2O$ maser action, a proposal first put forward by Hollenbach et al (1987). This proposal was taken up by Elitzur et al (1989) who presented a comprehensive model for maser emission from fast shocks, including detailed calculations of the shock structure and $H_2O$ pumping. In this model, the width of maser spots is identified with the thickness of the high-temperature plateau, $\sim 10^{13}$ cm for typical parameters. Individual maser features correspond to directions in the shock plane that attain the required line-of-sight velocity coherence in an otherwise turbulent medium, and were modeled as filaments with aspect ratios $\sim$5–50, typically. In a subsequent study, Elitzur et al (1991a) showed that the actual geometry in the plane of the shock is in fact irrelevant. The maser brightness temperature is determined by the length along the line of sight of the velocity coherent region and is largely independent of the shape in the transverse direction. To an observer in the plane, a disk maser appears identical to a filament whose length equals the disk diameter and whose aspect ratio is determined by this diameter and the pumping scheme. Typical aspect ratios derived from the $H_2O$ pumping model are in agreement with the values deduced from observations. Maser intensity is then determined by the dimension $l$ along the line of sight, i.e. the length of velocity coherent regions in the plane of the slab. Since brightness temperatures of $H_2O$ masers in star-forming regions display a

variation range of about three orders of magnitudes and since $T_b \propto l^3$, the lengths of velocity coherent regions vary by about a factor of ten in each source.

While collisional pumping of rotational levels appears adequate for explaining the masers, in principle other physical processes in the shocked environment could also play a role. An innovative pump mechanism was put forward by Strelnitskij (1980, 1984), involving collisions with electrons and neutrals at two different temperatures. This can lead to arbitrarily high brightness temperatures. While either relation between $T_e$ and $T_n$ is possible in principle for the operation of this mechanism, Strelnitskij advocated $T_e < T_n$, citing calculations by Bolgova (1981). Although it is difficult to devise models where this condition can be fulfilled, a high density two-temperature plasma where $T_e > T_n$ can be produced behind C-shocks, and Kylafis & Norman (1987) proposed that this may provide the explanation for $H_2O$ masers in star-forming regions. However, detailed calculations (Bolgova et al 1988, Elitzur & Fuqua 1989) confirm the Strelnitskij-Bolgova conclusion that two-temperature pumping of $H_2O$ can produce arbitrarily high brightness temperatures only when the electrons are cooler than the neutrals ($T_e < T_n$). In the reverse situation ($T_e > T_n$), the inversion is less efficient than what would be obtained by single-temperature pumping with either of the individual species alone. It thus seems unlikely that unrestricted two-temperature inversion could be incorporated into plausible models for $H_2O$ masers.

Another possible pump mechanism, proposed by Varshalovich et al (1983), involves vibrational energy exchange in $H_2$–$H_2O$ collisions. Although specific rate coefficients are not known, laboratory experiments show that processes of this type generally proceed at high rates. This is a natural process to consider in the context of the dissociative shock model because the $H_2$ is coming off the grains at highly excited vibration states. Collisions involving V-V transfer could then produce $H_2O$ at high vibrational states, followed by cascades to the ground vibration state, generating perhaps as much as a maser photon per vibrational excitation. Rates for some of the steps of this process are quite uncertain and it is not yet clear whether or not V-V transfer could play a significant role in $H_2O$ masers.

Dissociative shocks appear to provide an environment that adequately explains $H_2O$ maser observations. A survey of star-forming regions by Comoretto et al (1991) shows that $H_2O$ maser luminosities and overall mechanical shock luminosities are correlated in accordance with the model predictions. However, the specific evolutionary phase of the star-formation process associated with $H_2O$ maser action is not yet known. A telling example is provided by W49, the most luminous Galactic maser. High-

resolution observations by Welch et al (1987) show that the core of this star-forming region contains a 2 pc ring of at least ten distinct ultra-compact HII regions, each associated with at least one O star. The $H_2O$ maser emission is associated with one of those HII regions. Although the brightest, it is not clear what properties set this particular object apart from the other HII regions in the ring. Evidently, progress on this issue will be tied to overall progress and understanding of the star-formation process.

2.2.3 SUB-MILLIMETER MASERS For many years, the only strong $H_2O$ maser observed was the 22 GHz $6_{16} \rightarrow 5_{23}$ line. Most other $H_2O$ lines are strongly absorbed in the Earth's atmosphere and sporadic detections of two other transitions were confined to observations toward the Orion cloud with the Kuiper Airborne Observatory. The detected lines were $4_{14} \rightarrow 3_{21}$ at 380 GHz (Phillips et al 1980) and the para-$H_2O$ line $3_{13} \rightarrow 2_{20}$ at 183 GHz (Waters et al 1980, Kuiper et al 1984). The poor spatial resolution precluded reliable determination of the exact nature of the radiation in either case.

The absence of any other $H_2O$ transitions from the list of discovered astronomical masers stood in stark contrast with theoretical predictions: Beginning with the first model by de Jong (1973), every calculation concluded that there is nothing unique about the $6_{16} \rightarrow 5_{23}$ inversion and that many more transitions should be inverted (including $4_{14} \rightarrow 3_{21}$). Moreover, specific predictions for both late-type stars (Cooke & Elitzur 1985) and star-forming regions (Elitzur et al 1989) indicated that the photon luminosities of all masers are comparable. Then, all of a sudden a number of additional water maser transitions were detected in the span of a few months. The first discovery was the detection of the ortho-$H_2O$ 321 GHz $10_{29} \rightarrow 9_{36}$ transition by Menten et al (1990a) in both star-forming regions and late-type stars with photon luminosities comparable to those of the 22 GHz maser. This particular transition was not included in earlier theoretical studies because it involves levels much higher than those of the 22 GHz line. However, there is little fundamental difference between this transition and $8_{27} \rightarrow 7_{34}$, $6_{25} \rightarrow 5_{32}$, or $4_{23} \rightarrow 3_{30}$, for example, which were all predicted to be masers. Thus this line holds the distinction of being the first astronomical maser that was "almost predicted."

Calculations by Neufeld & Melnick (1990), which followed the 321-GHz discovery, had no problem explaining this maser emission utilizing the approaches developed earlier for modeling 22 GHz masers in late-type stars and star-forming regions and adding the required energy levels. At about the same time, Cernicharo et al (1990) used the IRAM 30-m telescope to re-observe the 183 GHz $3_{13} \rightarrow 2_{20}$ line of para-$H_2O$ under favorable weather conditions. Strong maser emission was detected in a variety

of 22 GHz sources. This important discovery prompted Neufeld & Melnick (1991) to add para-$H_2O$ to their previous extended study of ortho-$H_2O$ level populations in both late-type stars and star-forming regions. These calculations identified as the most promising candidate for new detection the 325 GHz $5_{15} \rightarrow 4_{22}$ line, which was promptly searched for and discovered by Menten et al (1990b) in several regions of active star formation. This is the first discovery of an astronomical maser line based upon specific theoretical prediction.

These rapid-fire developments confirm the theoretical claims that $6_{16} \rightarrow 5_{23}$ is but one of many maser lines and open up exciting new possibilities for maser research. Because different $H_2O$ maser transitions do not share common levels, they act as independent masers whose emission is a straight reflection of the pumping conditions. The studies by Neufeld & Melnick indicate that the ratio of maser emission in different lines is mostly determined by the temperature, as expected for collisionally-pumped saturated masers. The study of sources in different $H_2O$ maser lines could therefore help pinpoint the physical conditions in the sources. Hopefully, future orbiting facilities will enable detection of many more maser lines and enhance the usefulness of this promising tool.

## 2.3 *SiO*

2.3.1 LATE-TYPE STARS Observations by Jewell et al (1991) indicate that SiO could be the most prevalent type of circumstellar maser. The main limitation on additional detections is mostly instrumental. Interferometry by Colomer et al (1992) shows that observed spot sizes are rather compact, typically $\sim$0.1–0.6 AU for giants and $\sim$1–5 AU for supergiants. These sizes are much smaller than those obtained in previous observations (e.g. Lane 1982). It is not yet clear what is the cause for this discrepancy. Evidence continued to mount that, unlike OH and $H_2O$, this maser cannot reside in the expanding wind. Perhaps the most decisive argument with regard to this point is provided by the detection of $v = 3$ masers in stars whose mass-loss rates are among the lowest of all late-type stars: Alcolea et al (1989) detected $v = 3$ emission in RR Aql, R LMi, R Cas, and R Leo, whose mass-loss rates are only $7 \times 10^{-7}$, $7 \times 10^{-7}$, $6 \times 10^{-7}$, and $3 \times 10^{-8}\ M_\odot\ \mathrm{yr}^{-1}$, respectively (Lane et al 1987). At such low mass-loss rates, all optical depths for vibrational transitions are much less than unity in the wind region; even $v = 1 \rightarrow 0$ transitions are optically thin under such circumstances, so every transition to the $v = 3$ state fails to become optically thick by many orders of magnitude and inversion is impossible. This problem is avoided only if the masers reside in a region whose density is altogether unrelated to the mass-loss rate.

The lack of association between the expanding wind and SiO maser

activity is reflected in a number of observational properties (Nyman & Olofsson 1986). Stellar mass-loss rates and SiO photon fluxes are uncorrelated. The velocity range spanned by SiO features is very similar in different sources and poorly correlated with the expansion velocity of the circumstellar shell. This implies that in all stars, the masers are located in regions of similar velocity structure, which apparently bears no relation to that of the wind. Instead, SiO maser emission originates in large blobs, or emission cells, that form in the *extended atmosphere*—the region between the photosphere and the dust formation point. Cell lifetimes are typically a few months and in the case of regular variables can be as long as one-half to one period. A polarization map of R Cas, produced by McIntosh et al (1989), is presented in Figure 1 and provides an excellent illustration of the structure and overall properties of SiO masers. It shows that the emission originates in separate cells, each one characterized by distinct radial velocity, linear polarization, and polarization position angle, the last property presumably related to the orientation of the cell's magnetic field. SiO masers thus provide the opportunity for direct study of the stellar surface, since time monitoring of single cells can provide detailed information on motions and magnetic fields in the extended atmosphere. The only attempts at polarization monitoring were performed so far with single dishes and thus suffered from large uncertainties in the identifications of single cells. These problems can be overcome by time monitoring of spatially resolved polarized cells. Although difficult, these are most worthwhile observations.

Circular polarization at the several percent level was detected by Barvainis et al (1987) in five out of six stars observed. The detections imply that the Zeeman splitting must be at least comparable to the linewidth, which for SiO requires magnetic fields of a few tens of gauss. The strong surface fields have important consequences for the structure and dynamics of the SiO emitting region. The magnetic energy density exceeds the thermal energy density and the field is thus the dominant force in determining the kinematics of maser cells. McIntosh & Predmore (1991) extended linear polarization measurements up to $J = 3 \rightarrow 2$ masers and showed that the polarization *increases* with the $J$ value of the transition. This trend (rather, polarization *decrease* as $J$ decreases) could be due to Faraday rotation, but detailed calculations are not yet available. These observations also provide conclusive evidence that masers involving different rotation levels in the same vibration state originate in the same volume of gas: In Mira, all three $v = 1$ masers involving $J \leq 3$ show excellent correlations in velocity features and they also share the same polarization position angle. The opposite conclusion reached by Lane (1982) and Jewel et al (1987) about the spatial origin of different masers can be attributed to the varia-

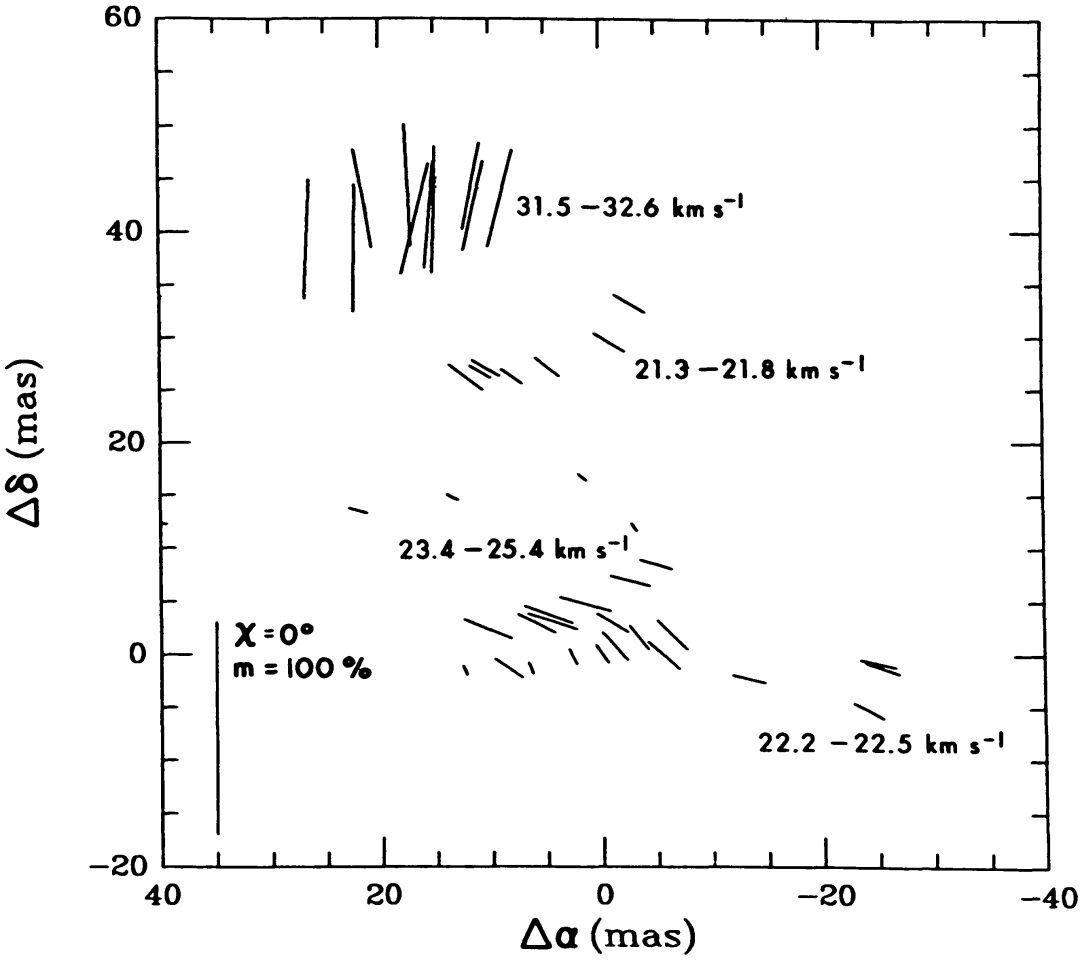


*Figure 1* Spatial polarization map of R Cas, produced in the $v = 1$, $J = 1 \rightarrow 0$ transition by McIntosh et al (1989) from a combination of VLBI mapping and single dish polarimetry data. The lines indicate the locations of various emission features and the numbers listed next to each group of lines provide the velocity range of the emission. For each line, the length is proportional to the fractional polarization and the orientation denotes the polarization position angle. The scale is provided at the lower left corner, which displays a line corresponding to 100% linear polarization at a position angle of 0°. At the assumed distance to R Cas of 266 pc, a linear dimension of $8 \times 10^{13}$ cm (approximately the stellar diameter) is equivalent to 20 milliarcsec.

bility of SiO masers, since both studies compared profiles taken at different times. It is probably significant that Jewell et al found that the profiles of $J = 6 \rightarrow 5$ and $5 \rightarrow 4$, observed in the span of a few days, were closely similar, but that both were different from the profile of $J = 2 \rightarrow 1$ which was observed two months later.

Long-term variability observations reveal conflicts with basic requirements of radiative pumping. SiO masers display periodic variations correlated with the visual light curve in many sources, but in most cases SiO lags in phase of up to $\sim 0.2$ behind the visual maximum (Clark et al 1984,

Nyman & Olofsson 1986, Martinez et al 1988). SiO variability therefore conflicts with radiative pumping by stellar photons. There appears to be a good agreement between variability of SiO and IR, which is also lagging behind the visual light curve in many sources. This indicates that the detected IR radiation does not originate from the photosphere and that both SiO and IR emissions originate from the same region in the extended atmosphere. Therefore, the radiation that dominates the observed spectrum at IR wavelengths cannot trigger SiO inversion by mechanisms that rely on directionality of pump photons (Deguchi & Iguchi 1976, Bujarrabal & Rieu 1981, Alcolea et al 1989), because this requirement is not met. Since this mechanism provides the only viable radiative pumps, pumping is collisional rather than radiative. Indeed, there is no correlation at all between the average SiO and IR amplitudes; in the sample of Nyman & Olofsson (1986), the two stars that had by far the largest dynamic ranges in SiO emission were among those displaying the smallest IR variations. Model calculations by Lockett & Elitzur (1991) show that the dominant pump mechanism in SiO masers is indeed collisions with neutral particles at $T \sim 120$ K and $n \sim 10^9$ cm$^{-3}$. These conditions are similar to those required for condensation of dust grains, so the turnoff of SiO emission at larger radii could be attributed in part to the disappearance of silicon from the gas phase due to its incorporation into the grain material. SiO maser activity is then the immediate predecessor of grain condensation. Muchmore et al (1987) point out that SiO formation may cause a cooling instability. Although some technical aspects of this proposal require checking by more detailed calculations, it raises some interesting possibilities: SiO cooling could trigger a two-phase instability resulting in the formation of clouds imbedded in a rarefied medium—the SiO maser emission cells. The clouds' lower temperatures and higher densities make them prime locations for initiating dust condensation and mass ejection. If this is the case, mass loss is initiated in large blobs rather than in a spherically symmetric fashion. The wind structure is then patchy near the star, in the $H_2O$ and OH main-lines maser regions, becoming smooth further out, in the OH 1612 MHz maser region, as the blobs expand. Though highly speculative, the overall trends predicted by this scenario are in good agreement with the observations of the various masers.

The general correlation trend of SiO and IR intensities can be attributed to the fact that both are related to a similar type of activity in the same region of the extended atmosphere, as indicated also by their correlated variability. Indeed, Hall et al (1990) find that a reliable indicator for SiO detection is large optical variability. The phase lags relative to visual emission observed in some stars indicate that the variations of both SiO and IR radiations reflect temperature changes caused by variations in the

local heating rate in response to the underlying stellar pulsation. When heating is dominated by radiative processes, the temperature varies without any phase delay and all three components (visual, IR, and SiO) vary in unison. When variations in the heating rate are dominated by mechanical effects, such as propagating shock waves for example, the SiO and IR lag behind the visual by a few months. Both types of variability are observed, although it is not clear why any given star should display one type rather than the other. No theoretical models have yet been constructed to explain this behavior even for IR radiation, although this phenomenon is considerably simpler and involves less details than SiO maser emission. The great complexity of extended atmospheres makes detailed studies difficult. SiO masers thus provide a powerful probe of a complex and interesting environment.

2.3.2 STAR-FORMING REGIONS Two ingenious modeling attempts of the Orion SiO maser emission, described in Section 5.4, resulted in the most detailed description yet of a circumstellar disk around a young star. Extensive surveys of other star-forming regions attempting to detect additional SiO masers met with limited success. New sources were discovered only in Sgr B2 and W51 (Hasegawa et al 1986, Fuente et al 1989). Each of the detected sources presents a set of unique properties that call for a separate modeling effort. In contrast with late-type stars, the conditions required for the operation of SiO masers are met in star-forming regions only on rare occasions.

## 2.4 $CH_3OH$

The latest species to join OH, $H_2O$, and SiO as a strong, widespread maser is methanol, also known as methyl alcohol and wood alcohol. The richness of the methanol spectrum and the large number of lines detected in interstellar space make the task of mere organization and classification a difficult one. Well over 200(!) lines in the frequency range between 834 MHz and 360 GHz have been detected to date. Over twenty of those display maser emission, detected in more than a hundred star-forming regions. The first detection of a $CH_3OH$ maser involved emission from the $J_{k=2} \rightarrow J_{k=1}$ series of the $E$ species, discovered toward Orion by Barrett et al (1971). The onset of rapid progress in $CH_3OH$ maser detections can probably be identified with the discovery of the $9_2 \rightarrow 10_1$ $A^+$ transition around 23 GHz (Wilson et al 1984). Both absorption and emission features were detected in a number of sources, and a very narrow ($\sim 0.3$ km s$^{-1}$), bright feature toward W3(OH) provided evidence for maser emission. This was followed by a continuous stream of new discoveries of maser emission in various cm- and mm-wave transitions. The latest discovery involves widespread, strong maser emission in the $5_1 \rightarrow 6_0$ $A^+$ transition at 6.6 GHz

(Menten 1991b). Except for the 22 GHz $H_2O$ maser, this is the strongest line detected in the interstellar medium so far. For example, its peak flux density in W3(OH) is 3880 Jy, about fifteen times higher than for OH in the same source (Garcia-Barreto et al 1988).

A comprehensive review of $CH_3OH$ masers has been presented by Menten (1991a). A scheme that divides methanol maser sources into two classes was put forward by Batrla et al (1987) and seems to accommodate properly all the discoveries made since its inception. According to this scheme, Class I sources are characterized primarily by maser action in the $J_2 \rightarrow J_1$ $E$ series at 25 GHz (currently including $J = 2$–9) and enhanced *absorption* at the $2_0 \rightarrow 3_{-1}$ $E$ 12 GHz transition. There is no association between Class I masers and any currently known compact IR or radio continuum sources, and they are definitely not coincident with either OH or $H_2O$ masers. Class I methanol masers may arise when mass outflows interact with ambient high density material (Plambeck & Menten 1990). The salient feature of Class II sources is strong $2_0 \rightarrow 3_{-1}$ $E$ 12 GHz emission, in marked contrast with the absorption that this transition displays in Class I sources. The newly discovered $5_1 \rightarrow 6_0$ $A^+$ 6.6 GHz transition appears to display the same pattern—absorption in Class I sources and strong maser emission in Class II sources. Class II sources are coincident with HII/OH regions; the methanol maser region is very compact and its small scale structure is very similar to that of the OH masers. A composite map of W3(OH) by Menten et al (1988), presented in Figure 2, shows a remarkable overall similarity between the distributions of OH and methanol masers. Most maser spots are clustered in what appears to be a ring around, approximately, the region's midsection, irrespective of the maser species or transition involved. The agreement applies to both spatial distribution and velocities, and it strongly suggests that both OH and methanol maser actions arise from similar clumps.

Pump mechanisms for either class have not yet been worked out in detail. A general argument that seems to explain some observable trends involves collisional excitations for certain $E$ transitions in Class I sources (Walmsley et al 1988). Because the propensity of collisions is to favor final states with the same $k$-value as the initial state, collisions at moderate temperatures will tend to overpopulate the $k = -1$ ladder. This produces inversion of $4_{-1} \rightarrow 3_0$ at 36 GHz and $5_{-1} \rightarrow 4_0$ at 84 GHz, and "anti-inversion," or "overcooling," of $2_0 \rightarrow 3_{-1}$ at 12 GHz. Both results are in agreement with observations of Class I sources. A similar simple analysis can be performed for $A$-methanol whose ground state is the $J = K = 0$ level, leading to an overpopulation of the $K = 0$ ladder. The first two transitions that can have inverted populations are the 44 GHz $7_0 \rightarrow 6_1^+$ and 95 GHz $8_0 \rightarrow 7_1^+$, as observed by Haschick et al (1990), while $5_1 \rightarrow$

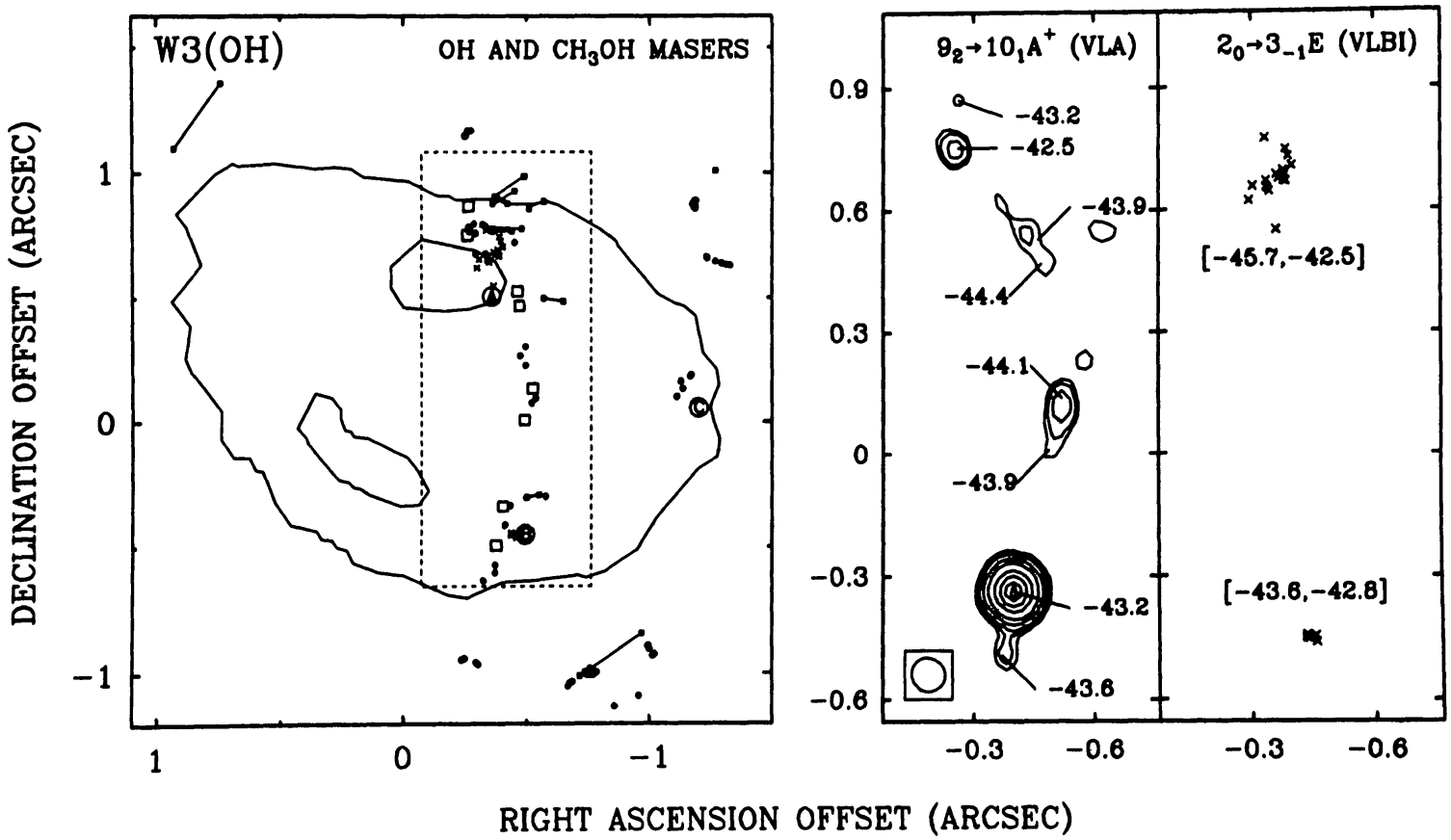


*Figure 2* A composite map of OH and $CH_3OH$ masers in W3(OH) (Menten et al 1988). In the left panel, contour lines mark the 10% and 70% levels of 23 GHz continuum emission. OH 1665 MHz masers are marked with filled circles and Zeeman pairs of 6035 MHz masers in the excited $^2\Pi_{3/2}(J = 5/2)$ state are shown as filled squares connected by lines. Letters *A*, *B*, and *C* mark the positions of the emission complexes in the 4765 MHz transition of $^2\Pi_{1/2}(J = 1/2)$. Positions of $CH_3OH$ masers are marked by crosses for $2_0 \rightarrow 3_{-1}$ *E* spots and open squares for $9_2 \rightarrow 10_1$ $A^+$ features. A dashed rectangle circumscribes the region containing methanol maser emission and blowup maps of this area are shown in the right two panels, one for each of the maser transitions. Differences in observing techniques are reflected in the appearance of these two maps. In the velocity-integrated VLA map, LSR velocities of individual $9_2 \rightarrow 10_1$ $A^+$ emission features are indicated and the beam is shown to the lower left. The VLBI map presents individual positions of $2_0 \rightarrow 3_{-1}$ *E* spots and the velocity range is indicated in brackets.

$6_0A^+$ at 6.6 GHz—the strongest $CH_3OH$ maser in Class II sources—is anti-inverted, again in agreement with observations (Menten 1991b). Therefore, although detailed calculations have not yet been performed, it seems likely that Class I masers may be collisionally pumped. There are no similar arguments regarding Class II masers. The high luminosities of the 6.6 and 12 GHz lines indicate that the methanol abundance in these sources must be rather high, a problem almost as challenging as understanding the pump mechanism itself (Batrla et al 1987). The close association with OH masers, both in the ground and excited states, suggests that the inversions of all these maser transitions require similar physical conditions, an issue that can be settled at a reasonable level of certainty by combined proper motion measurements of OH and methanol. This underscores the important role that methanol masers can play in the understanding of HII/OH regions.

## 2.5 $NH_3$

The first indication of possible $NH_3$ maser action in interstellar space came in a study by Wilson et al (1982). They observed the inversion doublet transitions in the four lowest possible metastable states $(J, K) = (1, 1)$, $(2, 2)$, $(3, 3)$, and $(4, 4)$ toward W33 and noted an anomalous behavior in the $(3, 3)$ doublet. While the three other lines, corresponding to para-$NH_3$, appeared only in absorption, this ortho-$NH_3$ line displayed only emission. They concluded that either the excitation temperature of $(3, 3)$ was considerably higher than that of the para species or the population in these doublet levels was slightly inverted. Subsequent VLA mapping of the $(3, 3)$ $^{15}NH_3$ line in the ultra-compact HII region IRS 1 in NGC 7538 by Johnston et al (1989) confirmed the maser nature of the emission and showed that it arises from many discrete clumps, with the brightness temperature of the most intense feature exceeding 5200 K. Although the maser spots have different positions, the $^{15}NH_3$, $H_2CO$, and OH (1665 MHz) emission probably all originate in a common highly clumped compact region in front of the HII region.

By now, maser detections have been extended to inversion transitions of nonmetastable states of both ortho-$NH_3$ and para-$NH_3$. The first display of unambiguous maser characteristics came with the discovery of maser emission in $(J, K) = (9, 6)$ by Madden et al (1986). The spectrum showed intense, narrow (0.5–1.5 km $s^{-1}$) emission features toward several star-forming regions. An interesting finding is that in W51, the velocities of some of the strongest $H_2O$ masers correspond to each of the $NH_3$ $(9, 6)$ velocities. Time variability for $NH_3$ masers was first noted by Madden et al (1986), with a more definitive case for variability obtained in subsequent observations by Madden et al (1988) and Wilson & Henkel (1988).

Pumping of the $NH_3$ masers is a difficult problem. With the exception

of the $(J, K) = (3, 3)$ line, all the masers occur in nonmetastable states, which tend to decay rapidly to the metastable levels on the corresponding $K$-ladders. It is not clear how to support sufficient populations at levels with such short lifetimes, located more than 1000 K above ground in some cases. Equally puzzling is the lack of a clear pattern in the inversions and why certain transitions are inverted while others are not. The potential significance of IR vibrational excitations was mentioned in two independent studies (Brown & Cragg 1987, Mauersberger et al 1987), but detailed calculations are yet to be presented.

## 3. PHENOMENOLOGY—EXTRAGALACTIC MASERS

Great progress has been made in studies of extragalactic OH, $H_2O$, and $H_2CO$. The last species is unique in that currently, more extragalactic (four) than Galactic $H_2CO$ maser sources have been detected. Most work on extragalactic masers has concentrated on studies of OH and $H_2O$, and these are the species that will be covered here.

### 3.1 *OH; Megamasers*

A new class of extragalactic OH sources was discovered with the detection of broad OH main-line maser emission from IC 4553 with an unprecedented isotropic luminosity, $\sim 10^3\, L_\odot$ (Baan et al 1982). By comparison, the isotropic luminosity of W3(OH), the prototype Galactic HII/OH region, is only $\sim 10^{-5}\, L_\odot$, that of the most luminous Galactic HII/OH region $\sim 10^{-3}\, L_\odot$. Thus IC 4553 is almost a million times more luminous than any OH maser source observed in the Galaxy, hence the name *megamaser*. By now, almost fifty megamasers have been detected, ranging in redshift up to $z = 0.17$; a comprehensive review was presented by Baan (1991). In spite of their spectacular isotropic luminosities, the OH brightness temperatures of megamasers are rather moderate, only $\sim 10^6$–$10^7$ K, comparable to those of the radio continuum at the same wavelengths. The OH maser emission of megamaser galaxies appears to be well explained by a simple model, first proposed by Baan & Haschick (1984) and Baan (1985): The maser emission is a low-gain amplification of the galactic-nucleus radio continuum by intervening molecular material. In IC 4553 the continuum and maser intensities are comparable and the amplification factor is only $e^\tau \sim 2$, corresponding to a gain of $\tau = 0.7$ and an inverted OH column density of $\sim 6 \times 10^{13}$ cm$^{-2}$. A comparison with typical extragalactic OH absorption column densities, $\sim (3\text{–}12) \times 10^{15}$ cm$^{-2}$ (Rickard et al 1982), shows that the required inversion is quite modest. The amplifying material resides in molecular clouds, similar to

those found in our own galaxy, that populate a nearly edge-on rotating disk around the nucleus. The high isotropic luminosity of the OH lines then does not reflect any exceptional circumstances since the inversion does not require unusual conditions.

Interferometric mapping provides strong support for this proposal. In all sources where such observations are available for both radio continuum and OH maser lines, the agreement in the superposition of the two has been confirmed; some caution must be exercised, though, since the number of cases is still limited and poor spatial resolution can occasionally lead to somewhat inconclusive results, as in the case of Mrk 273 (Schmelz et al 1987). The apparent gains, obtained from ratios of overall fluxes of maser lines and continuum at 18 cm, are rather weak. Chapman et al (1990) find that for 15 megamaser galaxies, the apparent gains range from 0.03 to 5.4 with a mean value of 1.0. Similar conclusions were reached by Henkel & Wilson (1990). Estimates of the fraction of the continuum source covered by OH clouds in various megamasers yield values in the range $\sim$0.1–0.01 (Henkel & Wilson 1990). The number of amplifying clouds is between 30 and 1000 and their volume filling factor is $\sim 10^{-3}$–$10^{-4}$ pc$^{-3}$ (Baan 1991).

The only pumping agent that can plausibly permeate large galactic volumes is dust IR radiation. Indeed, megamaser galaxies are extremely powerful infrared emitters, with IR luminosities in excess of $10^{11}$ $L_{\odot}$. A quadratic relation between OH and IR luminosities of megamaser galaxies was first noted by Martin et al (1988) and Baan (1989), and supported by subsequent observations. The extension of this correlation to extreme IR luminosities provides the basis for a suggestion of powerful (giga-) masers at early epochs ($z \sim 2$) of the evolution of the Universe (Burdyuzha & Komberg 1990). The IR luminosity distribution of all OH galaxies shows that those displaying absorption are clustered toward the lower luminosity end while megamasers occur at the higher end (Baan 1989, 1991). The distributions of the two groups are almost mutually exclusive, reflecting in all likelihood a separation between low and high effective dust temperatures. This trend is in agreement with modeling of OH main-line emission from late-type stars, whose line ratios appear similar to those of megamaser galaxies. It also indicates that the distribution of molecular clouds around the nucleus could be similar in all OH galaxies and that their different OH signatures arise from differences in dust properties. When the dust is not sufficiently warm to invert the main lines, absorption of the nuclear radio continuum produces OH absorption features. Warmer dust and a steep IR spectrum lead to inversion and background amplification, and the galaxy appears as a weak-gain, high-luminosity megamaser. Quite possibly, the key to the entire megamaser phenomenon could be the galactic IR, rather than OH, properties.

Detailed theoretical modeling of megamasers is not yet available; published results only involve studies that can be considered preliminary groundwork (Burdyuzha & Vikulov 1990). In fact, theoretical calculations could be hard pressed to improve much upon the basic points deduced thus far. Observations are limited to spatial resolutions that do not allow for detailed modeling of individual clouds, and there are no prospects for any useful degree of interferometric resolving power with Earth-confined baselines. As long as space VLBI is not available, model calculations will have to involve, by necessity, statistical averaging over many clouds, which are likely to have different properties for various lines, reducing the model's predictive power.

In spite of the spectacular overall luminosities, the basic requirements for OH emission from megamaser galaxies are neither extreme nor unusual and can certainly be expected to exist, and may even be widespread, within our own Galaxy. Such radiation may have gone unnoticed in Galactic sources because weak background amplification need not produce outstanding emission on the smaller scales of Galactic radio sources and individual molecular clouds. An important discovery in this regard is the detection of spatially extended anomalous OH emission in Galactic star-forming regions by Mirabel et al (1989). This OH emission is similar to, although much weaker than, that produced by extragalactic megamasers; line ratios are similar and the emission is spread over regions that are a few parsecs in size. If the similarity with megamasers holds, further studies of these sources could provide useful, more restrictive constraints on theoretical modeling.

OH megamaser emission probes a certain evolutionary stage favorable for this phenomenon, which in all likelihood is related to the IR signature of the galaxy. The identification of this stage in terms of various phases of galactic evolution is less clear. Two classes of active galaxies have been mentioned most often in association with megamasers: Seyfert and starburst galaxies. However, detailed analysis of the prototype megamaser, IC 4553, shows that although it shares properties of both, it does not fit neatly into either of these two categories (Norris 1985). It must be noted, though, that the distinction between these two classes is becoming somewhat blurred as more is learned about starburst galaxies, and it can be hoped that megamaser studies will help further understanding of this important issue.

## 3.2 $H_2O$

Extragalactic $H_2O$ maser sources divide into two classes. The first one includes masers that closely resemble Galactic star-forming regions, located outside nuclei of nearby systems (distances less than $\sim$3 Mpc).

Fourteen sources have been detected by now; detailed summaries and tabulations are available in Moran et al (1991) and Greenhill et al (1990). The latter authors also present detailed VLBI mapping of the best studied source in this class, the HII region IC 133 in M33. These high-resolution observations affirm the similarity of this source to W49—a point further illustrated by a map presented by Greenhill et al that shows how W49 would appear at the distance of M33. The relative narrowness of the velocity range of maser emission in IC 133 is attributed to the disparity in intensities between high- and low-velocity components of $H_2O$ masers: The relatively low intensity of high-velocity features in W49 would make them unobservable at the distance of M33.

The other class of $H_2O$ masers was discovered by Dos Santos & Lepine (1979) with the detection of strong 22 GHz emission from NGC 4945, a bright edge-on spiral galaxy. At an assumed distance of 4 Mpc, the isotropic luminosity is $\sim 85\ L_\odot$, almost two orders of magnitude more than W49 at its strongest phase. Subsequent discoveries brought the number of such extragalactic $H_2O$ masers to nine. The most luminous ones were found in NGC 4258 and NGC 1068 (isotropic luminosities of 120 and 350 $L_\odot$, respectively) by Claussen et al (1984), and in NGC 3079 (isotropic luminosity of 520 $L_\odot$) by Henkel et al (1984) and Haschick & Baan (1985). Unlike the former class of extragalactic masers, these $H_2O$ masers occur at the nuclei of distant galaxies (distances ranging to $\sim 16.5$ Mpc). The linewidths of single features ($\gtrsim 5$ km s$^{-1}$) and the velocity extent of the emission (up to $\sim 600$ km s$^{-1}$) are larger than typical values for Galactic $H_2O$ masers. VLA mapping by Claussen & Lo (1986) of the masers in NGC 4258 and NGC 1068 constrain their locations to regions with spatial extent less than 1.3 and 3.5 pc, respectively, at the center of each galaxy. They conclude that the luminous maser emission originates in very dense molecular gas clumps in the immediate vicinity of a central source with mass outflow. The underlying assumption of this proposal is that in analogy with Galactic star-forming regions, the $H_2O$ masers are generated by the interaction of a powerful outflow with the surrounding medium, only in this case the wind originates from the nucleus of a galaxy rather than a young star. Luminous $H_2O$ masers are then associated with activity at the nuclei of galaxies.

A different interpretation was proposed by Ho et al (1987), following observations toward NGC 253 and M51. These sources are spiral galaxies with active nuclei, and Ho et al also detected $H_2O$ maser emission toward both nuclei. But unlike the previous cases, $H_2O$ luminosities in both nuclei are quite moderate—0.2 $L_\odot$ in NGC 253 and 0.8 $L_\odot$ in M51. These luminosities, comparable to those of active Galactic star-forming regions, led Ho et al to suggest that the high luminosities observed in other galaxies

are simply the extreme end of a continuous distribution that includes the Galactic masers. The key then is the large sample rather than special gas properties in the nuclear environment; nuclei of galaxies are good places to find the most luminous masers simply because of the higher concentration of young stars.

Yet another interpretation was proposed by Haschick & Baan (1985) and Baan (1985). They suggest that, similar to OH megamasers, luminous $H_2O$ nuclear emission corresponds to low-gain maser amplification of the background continuum radio source. Subsequent interferometric observations of the nucleus of NGC 3079 showed that the maser source is coincident in angle with the nuclear compact radio source, in support of the proposal of background amplification (Haschick et al 1990). The $H_2O$ line profile and its central velocity suggest that the maser corresponds to a well defined region, which is moving outward relative to the molecular disk structure surrounding the nuclear source. There is evidence that the same outflowing molecular gas is also amplifying the OH main lines at 18 cm. From a comparison of the continuum and maser fluxes in NGC 3079, Haschick et al conclude that the maser gain is $\tau \sim 4$. This is comparable to the value $\tau \sim 8$ obtained for gains across shocked slabs with typical parameters required to explain Galactic $H_2O$ masers (Section 2.2.2). Luminous masers may thus result from the interception of the line of sight to the nucleus of the host galaxy by face-on shock fronts, similar to those generated in Galactic star-forming regions. The probability for such interceptions can be expected to correlate with the degree of nuclear activity, and this seems to fit well with the overall conclusions of Ho et al. This model may also incorporate the Claussen and Lo proposal that, on occasion, the masers may originate from a galactic wind, which could provide the shock trigger in some sources. Conceivably, all the salient features of the different schemes could be integrated into the background-amplification model.

Although the proposal invoking background amplification appears in reasonable agreement with the data, its conclusive verification will require a lot more observations which ultimately may have to involve space VLBI measurements. However, it is probably fair to conclude at this time that the pumping of extragalactic $H_2O$ masers need not involve any circumstances that are not encountered in Galactic sources.

## 4. PHYSICAL PROPERTIES

This section covers developments regarding fundamental physical properties of astronomical masers. Although most of the relevant studies are somewhat formal, spatial resolution has now reached the level that it

enables direct determination of fundamental maser properties. VLA observations of $H_2O$ masers in W Hya enabled Reid & Menten (1990) to reconstruct detailed properties of the maser source and the amplification process directly from the data with a minimal set of assumptions.

## 4.1 *Beaming*

Although the relevance of beaming to astronomical maser radiation was recognized rather early, its great significance in all geometrical configurations has not been fully appreciated in general. Maser radiation is highly beamed in all sources with an appreciable gain no matter what the geometry; the larger the gain, the more pronounced the beaming (Elitzur 1990). The beaming of maser radiation reflects the competition between different rays for inverted population. A particularly illuminating illustration of this competition is provided by an integral of motion, derived by Alcock & Ross (1985). For beamed radiation,

$$J_\nu = I_\nu(\mu_0)\frac{\Omega_\nu}{4\pi}, \qquad 1.$$

where $I_\nu(\mu_0)$ is the intensity along the direction $\mu_0$ of the local dominant ray, $J_\nu$ is the angle-averaged intensity, and $\Omega_\nu$ is the beaming solid angle. Beaming controls the behavior of astronomical maser radiation. Unfortunately, the beaming angle cannot be directly observed so its determination in any given source must rely on indirect methods. Reid & Menten (1990) determined beaming angles for $H_2O$ masers in W Hya from various constraints derived in the context of a complete construction of the maser model from observed properties. The derived values ($\Omega \sim 10^{-3}$–$10^{-4}$) are surprisingly small for masers that are unsaturated (the situation in this case), indicating that the spatial distribution of the masing molecules may be elongated in this source. Nedoluha & Watson (1991) proposed to determine $J$ from comparison of observed linewidths with the values expected from thermal motions, since line narrowing is controlled by $J$. The intensity $I$ (i.e. the brightness temperature) is directly determined from observations, and Equation 1 can then be utilized for the determination of $\Omega$. Although this method is hampered by uncertainties regarding linewidth analysis, it provides a new, independent means to constrain beaming angles.

4.1.1 CONVERTER VS AMPLIFIER DESCRIPTION A maser can be alternatively described as either an amplifier (of input radiation) or a converter (of pump events). Both descriptions are equally valid in *both the saturated and unsaturated regimes*, but there are reasons of convenience to prefer

one over the other in each case. The amplifier description of masers is based on the expression for intensity at an arbitrary point $\ell$

$$I_\nu(\ell) = I_\nu(\ell_0) \exp \tau_\nu(\ell, \ell_0), \qquad 2.$$

where $\tau_\nu(\ell, \ell_0)$ is the gain from some fiducial point $\ell_0$ along the ray path. Hence, every point in the maser can be considered the input source for maser radiation in every other location and the maser amplifies this radiation with an appropriate amplification factor. In an unsaturated maser the gain varies linearly with distance everywhere in the source and the amplification factor can be calculated at once. In a saturated maser, on the other hand, the gain's dependence on distance is linear in the unsaturated regions and logarithmic in the saturated zones. Thus the gain between two arbitrary points cannot be determined before the complete structure of the entire source has been determined. Therefore, in many applications the amplifier description is not particularly convenient for a saturated maser, even though it is perfectly valid.

The converter description can be obtained by inserting the beaming expression (Equation 1) into the equation of radiative transfer for the dominant ray, yielding

$$\frac{dI_\nu(\mu_0)}{d\ell} = \frac{h\nu\Phi_\nu}{\Omega_\nu} \frac{J_\nu}{J_\nu + J_s} \qquad 3.$$

(Elitzur et al 1991a). Here $\Phi_\nu$ is the rate for volume production (by the pump process) of inverted population that can interact with radiation at frequency $\nu$ and $J_s$ is the saturation intensity; specifically, $J_s = \Gamma/2B$, where $\Gamma$ is the loss rate of the maser system and $B$ is the Einstein $B$-coefficient of the maser transition. As the first factor on the right hand side indicates, essentially all the maser photons generated locally are channeled into the beaming angle $\Omega_\nu$ in the direction of the dominant ray. The second factor, $J_\nu/(J_\nu + J_s)$, is simply the efficiency with which the maser converts inversion-generating pump events into induced-emission photons, reflecting the only essential difference between unsaturated and saturated operation. In saturated regions ($J_\nu > J_s$) this conversion efficiency is unity and the intensity production rate can be obtained at once at every point. In unsaturated zones ($J_\nu < J_s$), on the other hand, the conversion efficiency depends on the energy density of the local radiation field and cannot be estimated before its structure in the entire source has been determined. Therefore, the converter description is not always useful in unsaturated masers, even though it is perfectly valid.

4.1.2 LARGE VELOCITY GRADIENTS The calculation of beaming angles (and brightness temperatures) of saturated masers is one of the most

challenging tasks for theory. Even in the seemingly simple case of an elongated cylinder, a proper, self-consistent treatment of the problem becomes quite involved (Elitzur et al 1991b). Similar calculations for the case when the maser particles participate in large-scale motions with velocity gradients have never been attempted. Masers in expanding winds have always been treated using the mean escape probability approach, in which the properties of the medium are averaged out. The wide variation of population difference in saturated regions makes simple averaging problematic for saturated masers. Still, a proper escape probability expression relating the emitted flux to the maser's overall gain can be developed even for saturated masers (Elitzur 1990). However, the maser escape probability involves the beaming angle, which remains unknown when ordered motions are important. Since a proper calculation must include the correct beaming angle, all past model calculations of masers in expanding winds are deficient (Lockett & Elitzur 1991). In spite of its significance for proper modeling of many sources, beaming of saturated masers in the case of large velocity gradients remains an unsolved problem.

## 4.2 *The Significance of Geometry*

Maser emission of the same species sometimes displays widely different properties in different environments. While a natural tendency is to attribute such disparities to differences in pumping schemes, developments in recent years indicate that kinematic-geometric factors could actually be dominant on occasion. The calculations of Cesaroni & Walmsley (1991; see Section 2.1.2) show that rotational excitations by far-IR radiation could be responsible for the OH ground-state main-line masers in HII/OH regions, similar to the situation in late-type stars. Line overlap appears to play a significant role in determining the pump efficiency. Different lines can be brought into overlap because of different molecular velocities in different regions due to large velocity gradients, a situation that can be called "global overlap," or because of large linewidths caused by turbulent motions, leading to "local overlap." The effects of global overlap appear to be negligible in general, those of local overlap can be significant on occasion (which seems to be the case in the Cesaroni & Walmsley results). The great disparity between the intensities and line ratios of main-line masers in HII/OH regions and late-type stars could perhaps be attributed to the widely different velocity fields, which may enable significant local overlap in the former environment but not the latter.

A similar situation exists for the $H_2O$ masers in late-type stars and in star-forming regions (Section 2.2). Again, the pump mechanism in the two environments are the same (i.e. rotational excitations in collisions with $H_2$ molecules) and physical conditions such as temperature, density, and $H_2O$

abundance are also similar. Still, the $H_2O$ masers in star-forming regions are considerably brighter. In all likelihood, this disparity is a reflection of the widely different geometries. Maser luminosity is directly related to the loss-line luminosity of the pump cycle. In late-type stars, the geometry of the maser region is determined by the velocity coherence properties of an expanding wind, leading to three-dimensional configurations. Large gains are impossible because they are associated with large optical depths for the loss lines, which lead to thermalization. In contrast, the masers in star-forming regions are produced in shocked regions whose slab-like geometry decouples maser action from thermalization, since the loss-line photons escape sideways. Maser intensity is then determined by the length along the line of sight of velocity coherent regions in the plane of the slab. These lengths can be considerably larger than the slab thickness, the dimension controlling the thermalization.

As these examples show, the geometry of the maser region can be at least as important as the pumping scheme in determining the maser brightness. Pumping considerations, even qualitative ones, must always take account of the source geometry.

## 4.3 *Fluctuations*

Recent OH maser observations of Galactic HII/OH regions by Clegg & Cordes (1991) show that the intensity amplitude in narrow frequency bands, much narrower than the thermal linewidth, exhibits fluctuations whose time scales range from a couple of minutes to an hour. The masers flicker over short time scales even though they display a high degree of stability in observations that average the intensities over long times. Standard rate equations for the maser levels determine the time behavior of the absorption coefficient $\kappa_\nu$ according to

$$\frac{d\kappa_\nu}{dt} = \Gamma[\kappa_{0\nu} - \kappa_\nu(1 + J_\nu/J_s)], \qquad 4.$$

where $\kappa_{0\nu}$ is the unsaturated absorption coefficient. The steady-state mean of $\kappa_\nu$ is obtained by setting $d/dt = 0$ and provides the standard expression used for describing observations that average over long times. Equation 4 implies that fluctuations around this steady-state mean decay at a rate $\Gamma$, the system loss rate (Elitzur 1991a). As a result, the maser effectively acts as a filter that passes only time-varying phenomena characterized by the time scale $1/\Gamma$, which is comparable to typical fluctuation times observed by Clegg & Cordes. In HII/OH regions, the OH abundance is controlled by the photodissociation of $H_2O$ molecules by the radiation of the central star. Fluctuations on time scale $1/\Gamma$ in the stellar radiation field may

then trigger the observed maser fluctuations (C. F. McKee 1991, private communication). It is perhaps significant that the one late-type star included in the observational program did not exhibit maser fluctuations. Maser fluctuation observations potentially provide a new probe of very detailed properties of the host environment.

The Clegg & Cordes discovery focuses attention on fundamental issues regarding the generation and statistics of astronomical maser radiation, issues that are important even when fluctuations are ultimately not produced in the observed radiation. The phenomenological equations for level populations and radiative transfer that form the basis for standard maser theory apply only to the steady-state solution, obtained by time averaging of the more fundamental equations. As evident from Equation 4, averaging times must exceed the mean fluctuation time, $1/\Gamma$. The distance traveled by the radiation during this time,

$$\lambda_c = c/\Gamma, \qquad 5.$$

defines a radiation correlation length. In steady state, averaging times that exceed $1/\Gamma$ imply averaging lengths that exceed $\lambda_c$. Maser amplification over one correlation length, measured by the gain $\kappa_\nu \lambda_c = \kappa_\nu c/\Gamma$, controls the degree of noise around the steady-state mean solution. These important issues require more study. Unfortunately, this problem has not been addressed since the pioneering studies of Litvak (1970) and Goldreich et al (1973). Missing is a first-principle solution of the astronomical maser problem that starts from the coupled equations for the radiation and density matrix and demonstrates, rather than assumes, the nature of the statistics.

## 4.4 *Polarization*

The electric field of maser radiation that propagates as a plane wave in a given direction, no matter what that direction is, has only two independent components, oscillating in the transverse plane. Yet maser radiation is produced in three independent states, corresponding to $\Delta m = +1, 0, -1$ transitions of the masing molecules. When the maser region is permeated by a magnetic field that provides a good quantization axis, these transitions produce three independent electric fields with well-determined directions with respect to the magnetic field. For Zeeman splitting smaller than the linewidth, the reduction of three modes to two is achieved because only waves that are launched with a proper phase difference between the three components of the generated $E$-field can propagate and get amplified (Elitzur 1991b). The relevant phase is determined by the angle between the magnetic field and the direction of wave propagation (i.e. the local dominant ray), and in turn determines the polarization of propagating modes. The resulting polarization corresponds to the solution obtained by Gold-

reich et al (1973). The polarization of steady-state maser radiation is thus fully determined by the beamed nature of the radiation (which implies that it can be described by plane waves), the independence of pumping into the different sub-states of the maser system, and the uniformity of the quantization axis direction. The polarization is independent of the degree of saturation or the $J$-values of the system spins. Indeed, the SiO polarization observations of McIntosh & Predmore (1991) indicate that, with the possible exception of Faraday rotation effects, polarization properties may be $J$-independent. The detailed nature of the mode selection process and the possible effects of fluctuations have not yet been studied. These issues are closely related to those mentioned in the last section.

A new mechanism for filtering individual circular polarization components was proposed by Deguchi & Watson (1986). The operation of this mechanism requires a large velocity gradient and Zeeman splitting comparable to the thermal linewidth, but does not require magnetic field gradients. Detailed mapping of W3(OH) in all four Stokes parameters by Garcia-Barreto et al (1988) shows that there are no detected features with purely linear or unpolarized emission that might have been identified as $\pi$ components. This conflicts with the theoretical results for polarization when the Zeeman splitting exceeds the linewidth, which otherwise seem applicable. Faraday rotation, which requires more theoretical studies, is a possible explanation.

### 4.5 *Background Amplification*

The potential significance of maser amplification of background radiation has been recognized in a number of sources, in particular extragalactic masers (Section 3). Various misconceptions that existed in the literature regarding background amplification by *saturated* masers are clarified when the effect of the background radiation on the maser structure is properly accounted (Elitzur et al 1991b).

## 5. MASERS AS ASTRONOMICAL TOOLS

Maser radiation provides an intense, collimated beacon that can serve as a probe for the source in which it was produced and the medium in which it is propagating. Some of the probed properties can be deduced even without modeling of the maser process itself. In such cases maser radiation provides a general astronomical tool, employed in the analysis of properties altogether unrelated to maser action per se. Some of the most exciting and significant developments in maser research in recent years involve techniques of this kind.

## 5.1 *Distance Measurements*

Distance determination can be considered one of the most, if not the most, difficult problems in astronomy. Only in the case of relatively nearby objects can distances be determined by purely geometric or kinematic methods, free of assumptions about "standard candle" properties. Proper motion measurements of $H_2O$ masers extend kinematic distance determinations to distances far beyond those possible with previous techniques. The advent of this method, pioneered by a group centered at the Harvard-Smithsonian Center for Astrophysics (Genzel et al 1981a,b; Schneps et al 1981), is arguably one of the most important developments in astronomical techniques of the past ten years or so. Among other sources, this method was used to model the proper motions of the $H_2O$ maser spots in Sgr B2(N), yielding a distance $R_0 = 7.1 \pm 1.5$ kpc to the Galactic center (Reid et al 1988). Maser proper motion measurements of distances to other star-forming regions can also be employed for determining $R_0$, when used in conjunction with kinematic distance estimates obtained from comparison of the source velocity with models for Galactic rotation. A review of various methods that can be used to determine $R_0$ is provided by Reid (1989), who concludes that the most reasonable current estimate is $R_0 = 7.7 \pm 0.7$ kpc.

With all the impressive accomplishments already attained with this new technique, the future could be even brighter. Higher frequency methanol masers hold the promise of higher accuracies because angular resolution improves with frequency. Proper motion measurements can also be extended to other galaxies. Indeed, the VLBI mapping the $H_2O$ masers in M33 by Greenhill et al (1990) determined some relative positions accurately enough to provide first-epoch measurements for proper motion studies. It can be expected that in the near future these measurements will provide the first ever kinematic-geometric measurement of distance to an extragalactic object, removing significant sources of error in the determination of the Hubble constant. No other astronomical technique currently available comes close to such a feat.

## 5.2 *Galactic Properties*

5.2.1 GALACTIC ROTATION The double-peak profile of 1612 MHz OH maser emission provides a unique signature for type II OH/IR stars, enabling easy identification. Because of their high radio luminosity, these masers can be detected throughout the Galaxy. A survey of OH/IR stars within one degree of the Galactic center by Habing et al (1983) resulted in the first actual detection of Galactic rotation in a stellar population near the center. The results show that the average radial velocity of stars varies

linearly with Galactic longitude, as expected in a rotation. From a model fit to the velocities Habing et al deduced the parameters of the rotation, and from dynamical considerations they derived the mass distribution near the center. The results are in good agreement with other determinations, based on quite different methods and assumptions.

5.2.2 GALACTIC MAGNETIC FIELD The Zeeman effect of a typical magnetic field in an HII/OH region (a few mG) splits the OH spectral lines by an amount exceeding the linewidth, producing pairs of right and left circularly polarized lines. The splitting is proportional to the magnitude of the magnetic field, whose value is thus a directly measurable quantity. In addition to the full magnitude of the *B*-field, OH Zeeman measurements yield the line-of-sight direction of the field, i.e. whether it points toward or away from the observer. The actual, full three-dimensional direction of the magnetic field is still undetermined. However, because the Earth is far removed from the Galactic center, the transformation of line-of-sight directions to Galactic coordinates yields meaningful information about the sense in which the field points at different Galactic locations.

Using this approach, Reid & Silverstein (1990) deduced field properties in 17 OH maser sources for which the Zeeman effect can be demonstrated convincingly. Their results, shown in Figure 3, display the striking effect that, of the 17 OH sources, 14 have line-of-sight *B*-field directions that point in the direction of Galactic rotation (clockwise in the figure); in only 3 sources is the direction opposite (counterclockwise) to the sense of the rotation. Were the distribution of *B*-field directions entirely random, the probability of obtaining this result would be only about 6%. Outside of 6 kpc from the Galactic center 9 of 10 line-of-sight *B*-fields point in the direction of Galactic rotation. The magnetic field structure implied by this map has large-scale features with the same line-of-sight direction that span arcs (or annuli) over many kiloparsecs. The results suggest that the magnetic field direction is largely preserved during contraction from interstellar densities ($\sim 1$ cm$^{-3}$), through those of giant molecular clouds ($\sim 10^3$ cm$^{-3}$), to those of OH masers ($\sim 10^7$ cm$^{-3}$) near newly formed massive stars, and that the Galactic magnetic field is the dominant force in the process of collapse toward stellar densities. OH Zeeman measurements provide a powerful technique that will undoubtedly become a major tool in Galactic studies.

## 5.3 *Interstellar Scattering*

Radio radiation propagating in the interstellar medium is subject to scattering by interstellar plasma. This scattering produces diffractive and refractive effects, induced by large-scale fluctuations in the density of free

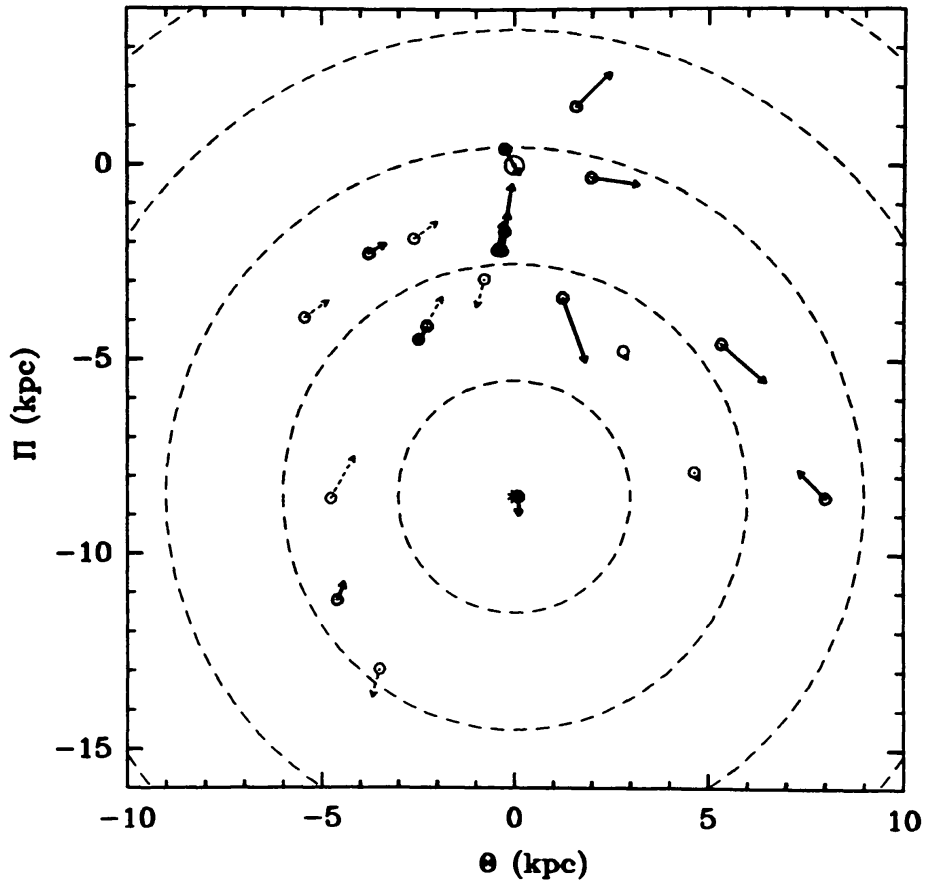


*Figure 3* OH mapping of the Galactic magnetic field, displaying the appropriate OH maser sources on the Galactic plane (Reid & Silverstein 1990). Locations of the maser sources are given by circles, and the full *B*-field magnitude and line-of-sight directions are indicated by the length and direction of the arrows, respectively. Sources with kinematic distance ambiguity have dashed arrows and are shown at both possible locations in the Galaxy. The Sun, indicated by the solar symbol, is at the origin of the plot ($\Pi = \Theta = 0$) and 8.5 kpc from the Galactic center, indicated by an asterisk at $\Theta = 0$, $\Pi = -8.5$ kpc. Galactocentric distances of multiples of 3 kpc are indicated by dashed circles.

electrons in the intervening medium. Maser spots provide compact input sources that are particularly suitable for observations of such scattering effects, which provide information on the power spectrum of the density fluctuations.

Angular sizes are broadened by scattering, so apparent images should increase with distance to the source. A correlation of maser spot angular size with source distance has been demonstrated for OH masers by Diamond et al (1988) and for $H_2O$ masers by Gwinn et al (1988a,b). Observed angular sizes vary with distance in general agreement with the theoretical

result for interstellar scattering by density fluctuations distributed according to the Kolmogorov spectrum. Estimates of the strength of the electron density fluctuations, obtained from the coefficient of the correlation relation, are in general agreement with values determined by other means. The predicted dependence on wavelength, $\lambda^{2.2}$, also seems to be borne out by the observations, as first noted by Moran et al (1973).

The $H_2O$ maser observations enabled measurement of another refraction induced effect. Large-scale density fluctuations produce deflections of source images, which should vary with time when the line of sight moves through the scattering medium. If a source moves at constant velocity, as along a ballistic trajectory in free space, refractive deflection will produce apparent wander in position about the actual trajectory. Limits on the wander of $H_2O$ maser spots in Sgr B2 and W49 were obtained from observations made at different epochs. In conjunction with size measurements, these limits constrain possible power-law spectra of the density fluctuations to indices consistent with the Kolmogorov value of 3.67. The constraints are not unique, however, as Gwinn et al (1988b) point out that an alternative explanation for the measured limits is a long-wavelength cutoff in the fluctuation spectrum at about $10^{13}$ cm. Future high resolution observations, especially with space VLBI, should make important contributions to this new and promising direction of research.

## 5.4 *Circumstellar Disk Structure*

Identifying circumstellar disks around newly formed stars and probing their structures are major challenges for astronomical observations. Using the Hat Creek millimeter array, Plambeck et al (1990) performed interferometric observations of the Orion SiO maser in the 86 GHz $v = 1$, $J = 2$–1 transition and obtained what is currently the best evidence for and the most detailed mapping of an expanding-rotating circumstellar disk. The map they produced, presented in Figure 4, suggests that the masers are distributed in a ring, presumably centered on the star itself, and the regular velocity pattern further suggests that systematic motions dominate the gas within the ring. Plambeck et al model these motions with an expanding-rotating disk, inclined with respect to the plane of the sky. Maser radiation recorded at each velocity channel has its origin in volume elements whose velocity projection along the line of sight matches the given value. Local conditions such as densities, temperature, etc, determine the maser volume emission rate $\Phi$. Along any cord through the disk the decline in $\Phi$ determines an effective length for a corresponding maser filament. A measure of this length $L$ is obtained in the model analysis from the integral of $\Phi$ along the line of sight, and the intensity is expected to scale as $L^3$. Contour plots of $L$ therefore identify the maser emission

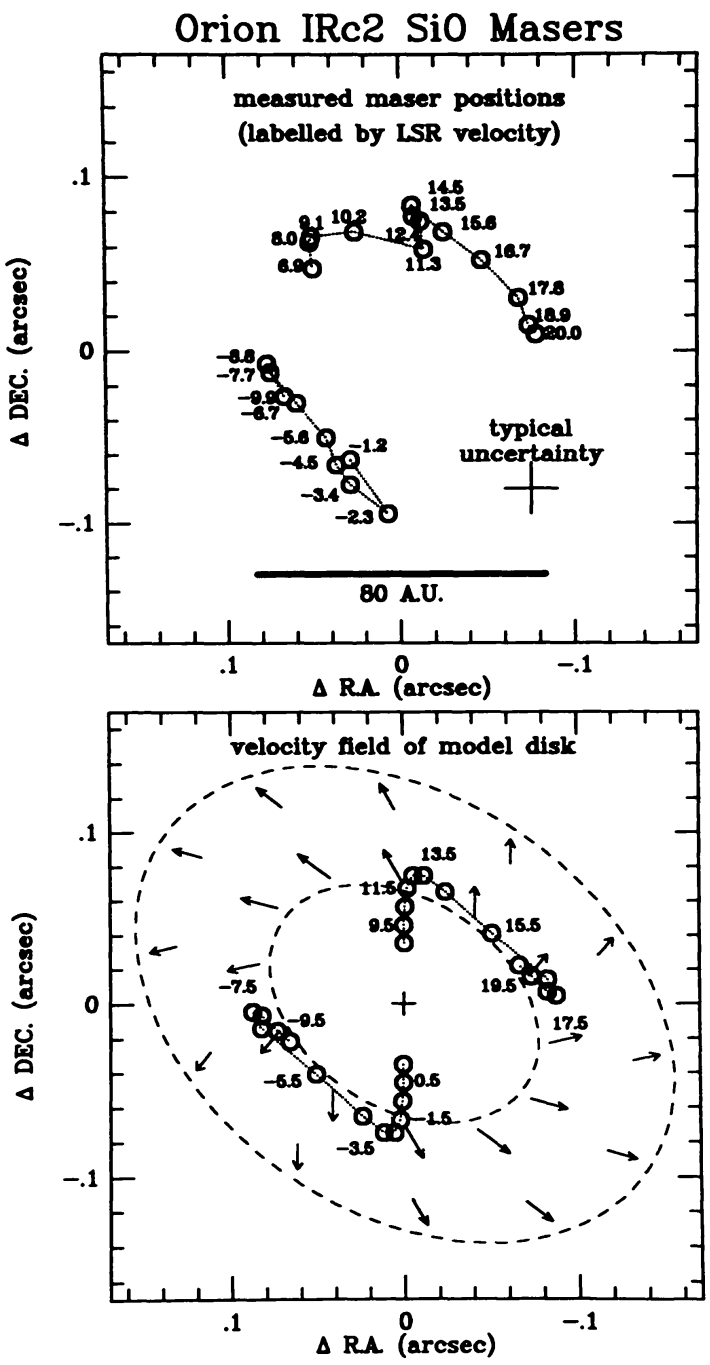


*Figure 4* Observations and modeling of the Orion SiO maser (Plambeck et al 1990). The top panel displays positions of the maser emission centroids as circles labeled by the appropriate LSR velocity in km $s^{-1}$, at 1.08 km $s^{-1}$ intervals. The bar at the bottom marks a linear scale of 80 AU at the distance to Orion. The bottom panel presents a plot of the model disk with the inner and outer boundaries indicated by dashed lines, the center by a cross, and the velocity field by arrows. The disk is inclined by 45° with respect to the line of sight; its SE edge, at the lower left corner, is nearest us.

regions for every velocity and their intensity-weighted centroids are the positions denoted by circles in the bottom panel of Figure 4. Emission spots extend beyond the dashed boundaries because the disk has a large thickness, equal to its inner radius. The preferred choices for the velocity field include a radial velocity similar to that in a gravitationally decelerated outflow and a tangential velocity field describing Keplerian rotation.

Polarization data analysis by Barvainis (1984) led to a similar model for the Orion SiO maser. In spite of some minor differences in details, there is a close agreement between the disk structures produced in the two models. It is remarkable that two studies that utilized completely different phenomena for such detailed modeling agree so well. This agreement enhances confidence in the basic premises of the two models and in the underlying theory that forms the basis for the two analyses. Maser observations currently provide the only astronomical technique capable of producing this level of detail in an object at the distance of Orion.

## 5.5 *Evolutionary Schemes for Late-Type Stars*

Maser emission in late-type stars results from coincidences among certain properties of the circumstellar environment. Such coincidences are a direct consequence of the detailed structure of the stellar surroundings, which in itself reflects the evolutionary stage reached by the star. This raises the interesting possibility that statistical analysis that treats maser stars as a stellar population will provide information, otherwise unavailable, about the final stages of evolution on the asymptotic giant branch.

This approach was taken by Baud & Habing (1983) who performed a comprehensive analysis of 1612 MHz maser stars using the rather complete survey of Baud et al (1981). The basic premise of the scheme they develop is that the OH maser properties are predominantly controlled by $\dot{M}$, which is directly related to the time spent in the OH emitting phase. They also demonstrate that at any given time, the mass-loss rate is inversely proportional to the residual mass of the stellar envelope. The initial phase of 1612 MHz maser emission occurs during an early stage of the wind development and is characterized by a relatively low mass-loss rate, $\gtrsim 3 \times 10^{-6}\ M_\odot\ \mathrm{yr}^{-1}$. As the stellar envelope loses mass, the mass-loss process accelerates until finally the star enters a superwind phase with $\dot{M} \geq 10^{-5}\ M_\odot\ \mathrm{yr}^{-1}$. This is a relatively short final burst of mass loss, leading to the formation of a planetary nebula. De Jong (1983) performed a similar analysis utilizing the same data and reached similar overall conclusions. He points out that although the mass-loss rate is higher for the superwind, most of the envelope mass is actually lost during the ordinary wind phase because of its much longer duration. Only about 1%

of stars are in the superwind phase at any given time, in agreement with Baud & Habing.

The studies of Baud & Habing and of de Jong were confined to the 1612 MHz OH maser stars. A much more ambitious, though somewhat less quantitative, scheme was proposed by Lewis (1989) for the evolution of all masers in the circumstellar shells of late-type stars. Similar to Baud & Habing, Lewis too uses the mass-loss rate, which he associates with the IR colors of the shell, as the primary indicator for the maser signature. According to his scheme, SiO, $H_2O$, and OH main lines and finally OH 1612 MHz masers are added one by one in a chronological sequence as the mass-loss rate increases. He argues that except for the 1612 MHz line, the masers disappear in the reverse order as the shell thickens. A novel feature of his proposed scheme is that the main lines reappear after the mass-loss process turns off and the shell is detached from the star, prior to the planetary nebula formation stage. Thus the main-line maser phase is bimodal in this scheme. Support for the basic premise of this chronological sequence comes from analysis of IR properties of a large sample of Mira variables by Stencel et al (1990). The stars in the sample were divided into six classes according to the colors and features of their IR spectra. Comparison with dust properties obtained in laboratory studies of grain formation and annealing suggests that these IR classes reflect the length of time the grains have been processed following formation, that is, the evolutionary stage of the circumstellar shell. There is a strong trend of evolution for various masers in different IR classes along the lines suggested by Lewis' chronological sequence.

Studies of evolutionary schemes provide a most interesting and exciting development in maser research. Masers are used as markers for late evolutionary stages of stars sometimes completely hidden by thick dust shells. Investigations of this nature will undoubtedly become a most important part of stellar evolution studies.

## ACKNOWLEDGMENTS

I thank W. Baan, D. Downes, K. Menten, J. Moran, M. Walmsley, J. Welch, and T. Wilson for providing most useful help with various developments covered in this review. The support of NSF grant AST-9016810 and an NRC research associateship are gratefully acknowledged.

*Literature Cited*

Alcock, C., Ross, R. R. 1985. *Ap. J.* 290: 433
Alcolea, J., Bujarrabal, V., Gallego, J. D. 1989. *Astron. Astrophys.* 211: 187
Baan, W. A. 1985. *Nature* 315: 26
Baan, W. A. 1989. *Ap. J.* 338: 804
Baan, W. A. 1991. In *Skyline: Proc. 3rd Haystack Conf.*, ed. A. D. Haschick, P. T. P. Ho, p. 45. San Francisco: Astron. Soc. Pac.

Baan, W. A., Haschick, A. D. 1984. *Ap. J.* 279: 541
Baan, W. A., Wood, P. A. D., Haschick, A. D. 1982. *Ap. J. Lett.* 260: L4
Barrett, A. H., Schwartz, P. R., Waters, J. W. 1971. *Ap. J.* 16: L1
Barvainis, R. 1984. *Ap. J.* 279: 358
Barvainis, R., McIntosh, G., Predmore, C. R. 1987. *Nature* 329: 613
Batrla, W., Matthews, H. E., Menten, K. M., Walmsley, C. M. 1987. *Nature* 326: 49
Baud, B., Habing, H. J. 1983. *Astron. Astrophys.* 127: 73
Baud, B., Habing, H. J., Matthews, H. E., Winnberg, A. 1981. *Astron. Astrophys.* 95: 156
Baudry, A., Diamond, P. J., Booth, R. S., Graham, D., Walmsley, C. M. 1988. *Astron. Astrophys.* 201: 105
Berulis, I. I., Ershov, A. A. 1983. *Sov. Astron. Lett.* 9: 341
Bloemhof, E. E., Reid, M. J., Moran, J. M. 1989. In *Physics and Chemistry of Interstellar Molecular Clouds*, ed. G. Winnewisser, J. T. Armstrong, p. 228. Berlin: Springer-Verlag
Bolgova, G. T. 1981. *Nauchn. Inf. Astrosovijeta AN SSSR* 47: 9
Bolgova, G. T., Makarov, S. V., Sobolev, A. M. 1988. *Astrofizika* 28: 405
Booth, R. S., Kus, A. J., Norris, R. P., Porter, N. D. 1981. *Nature* 290: 382
Bowers, P. F. 1985. In *Mass Loss from Red Giants*, ed. M. Morris, B. Zuckerman, p. 189. Dordrecht: Reidel
Bowers, P. F., Hagen, W. 1984. *Ap. J.* 285: 637
Brebner, G. C., Heaton, B., Cohen, R. J., Davies, S. R. 1987. *MNRAS* 229: 679
Brown, R. D., Cragg, D. M. 1987. *Aust. Phys.* 24: 184
Bujarrabal, V., , Rieu, N. Q. 1981. *Astron. Astrophys.* 102: 65
Burdyuzha, V. V., Vikulov, K. A. 1990. *MNRAS* 244: 86
Burdyuzha, V. V., Komberg, B. V. 1990. *Astron. Astrophys.* 234: 40
Cernicharo, J., Thum, C., Hein, H., John, D., Garcia, P., Mattioco, F. 1990. *Astron. Astrophys.* 231: L15
Cesaroni, R., Walmsley, C. M. 1991. *Astron. Astrophys.* 241: 537
Chapman, J. M., Cohen, R. J. 1986. *MNRAS* 220: 513
Chapman, J. M., Staveley-Smith, L., Axon, D. J., Unger, S. W., Cohen, R. J., et al 1990. *MNRAS* 244: 281
Clark, F. O., Troland, T. H., Pepper, G. H., Johnson, D. R. 1984. *Ap. J.* 283: 174
Claussen, M. J., Heiligman, G. M., Lo, K. Y. 1984. *Nature* 310: 298
Claussen, M. J., Lo, K. Y. 1986. *Ap. J.* 308: 592
Clegg, A. W., Cordes, J. M. 1991. *Ap. J.* 374: 150
Cohen, R. J. 1987. In *Circumstellar Matter*, ed. I. Appenzeller, C. Jordan, p. 229. Dordrecht: Reidel
Cohen, R. J. 1989. *Rep. Prog. Phys.* 52: 881
Cohen, R. J., Downes, G., Emerson, R., Grimm, M., Gulkis, S., et al. 1987. *MNRAS* 225: 491
Cohen, R. J., Baart, E. E., Jonas, J. L. 1988. *MNRAS* 231: 205
Colomer, F., Graham, D. A., Krichbaum, T. P., Ronnang, B. O., de Vicente, et al. 1992. *Astron. Astrophys.* In press
Comoretto, G., Brand, J., Catarzi, M., Cesaroni, R., Giovanardi, et al. 1991. In *Skyline: Proc. 3rd Haystack Conf.*, ed. A. D. Haschick, P. T. P. Ho. Provo: Astron. Soc. Pac.
Cooke, B., Elitzur, M. 1985. *Ap. J.* 295: 175
de Jong, T. 1973. *Astron. Astrophys.* 26: 297
de Jong, T. 1983. *Ap. J.* 274: 252
Deguchi, S. 1977. *Publ. Astron. Soc. Jpn.* 29: 669
Deguchi, S. 1982. *Ap. J.* 259: 634
Deguchi, S., Iguchi, T. 1976. *Publ. Astron. Soc. Jpn.* 28: 307
Deguchi, S., Watson, W. D. 1986. *Ap. J. Lett.* 300: L15
Diamond, P. J., Martinson, A., Dennison, B., Booth, R. S., Winnberg, A. 1988. In *Radio Wave Scattering in the Interstellar Medium*, ed. J. M. Cordes, B. J. Rickett, D. C. Backer, p. 195. New York: Am. Inst. Phys.
Dickinson, D. F. 1987. *Ap. J.* 313: 408
Dickinson, D. F. 1991. *Ap. J. Lett.* In press
Dos Santos, P. M., Lepine, J. R. D. 1979. *Nature* 278: 34
Elitzur, M. 1990. *Ap. J.* 363: 638
Elitzur, M. 1991a.*Ap. J. Lett.* 370: L45
Elitzur, M. 1991b. *Ap. J.* 370: 407
Elitzur, M., de Jong, T. 1978. *Astron. Astrophys.* 67: 323
Elitzur, M., Fuqua, J. B. 1989. *Ap. J. Lett.* 347: L35
Elitzur, M., Hollenbach, D. J., McKee, C. F. 1989. *Ap. J.* 346: 983
Elitzur, M., Hollenbach, D. J., McKee, C. F. 1991a. *Ap. J.* Submitted
Elitzur, M., McKee, C. F., Hollenbach, D. J. 1991b. *Ap. J.* 367: 333
Engels, D., Schmid-Burgk, J., Walmsley C. M. 1986. *Astron. Astrophys.* 167: 129
Fiebig, D., Gusten, R. 1989. *Astron. Astrophys.* 214: 333
Fuente, A., Martin-Pintado, J., Alcolea, J., Barcia, A. 1989. *Astron. Astrophys.* 223: 321
Garcia-Barreto, J. A., Burke, B. F., Reid, M. J., Moran, M. J., Haschick, A. D., Schilizzi, R. T. 1988. *Ap. J.* 326: 954
Genzel, R. 1986. In *Masers, Molecules and*

*Mass Outflows in Star Forming Regions*, ed. A. D. Haschick , p. 233. Westford, MA: Haystack Obs.
Genzel, R., Reid, M. J., Moran, J. M., Downes, D. 1981a. *Ap. J.* 244: 884
Genzel, R., Downes, D., Schneps, M. H., Reid, M. J., Moran, J., 1981b. *Ap. J.* 247: 1039
Goldreich, P., Keeley, D. A., Kwan, J. Y. 1973. *Ap. J.* 179: 111
Gordon, M. A. 1991. *Ap. J.* To be published
Green, S. 1980. *Ap. J. Suppl.* 42: 103
Greenhill, L. J., Moran, J. M., Reid, M. J., Gwinn, C. R., Menten, K. M., et al. 1990. *Ap. J.* 364: 513
Guilloteau, S., Omont, A., Lucas, R. 1987. *Astron. Astrophys.* 176: L24
Gwinn, C. R., Moran, J. M., Reid, M. J. 1988a. In *Radio Wave Scattering in the Interstellar Medium*, ed. J. M. Cordes, B. J. Rickett, D. C. Backer, p. 129. NY: Am. Inst. Phys.
Gwinn, C. R., Moran, J. M., Reid, M. J., Schneps, M. H. 1988b. *Ap. J.* 330: 817
Gwinn, C. R., Moran, J. M., Reid, M. J. 1991. *Ap. J.* Submitted
Habing, H. J., Olnon, F. M., Winnberg, A., Matthews, H. E., Baud, B. 1983. *Astron. Astrophys.* 128: 230
Hall, P. J., Allen, D. A., Troup, E. R., Wark, R. M., Wright, A. E. 1990. *MNRAS* 243: 480
Haschick, A. D., Baan, W. A. 1985. *Nature* 314: 144
Haschick, A. D., Menten, K. M., Baan, W. A. 1990. *Ap. J.* 354: 556
Hasegawa, T., Morita, K. I., Okumura, S., Kaifu, N., Suzuki, H., et al. 1986. In *Masers, Molecules and Mass Outflows in Star Forming Regions*, ed. A. D. Haschick, p. 275. Haystack Obs.
Henkel, C., Wilson, T. L. 1990. *Astron. Astrophys.* 229: 431
Henkel, C., Gusten, R., Downes, D., Thum, C., Wilson, T. L., Bierman, P. 1984. *Astron. Astrophys.* 141: L1
Herman, J., Habing, H. J. 1985a. *Phys. Rep.* 124: 255
Herman, J., Habing, H. J. 1985b. *Astron. Astrophys. Suppl.* 59: 523
Ho, P. T. P., Martin, R. N., Henkel, C., Turner, J. L. 1987. *Ap. J.* 320: 663
Hollenbach, D. J., McKee, C. F., Chernoff, D. 1987. In *Star Forming Regions*, ed. M. Peimbert, J. Jugaku, p. 334. Dordrecht: Reidel
Jewell, P. R., Dickinson, D. F., Snyder, L. E., Clemens, D. P. 1987. *Ap. J.* 323: 749
Jewell, P. R., Snyder, L. E., Walmsley, C. M., Wilson, T. L., Gensheimer, P. D. 1991. *Astron. Astrophys.* 242: 211
Johnston, K. J., Stolovy, S. R., Wilson, T. L., Henkel, C., Mauersberger, R. 1989. *Ap. J. Lett.* 343: L41
Kuiper, T. B. H., Rodriguez Kuiper, E. N., Swanson, P. N., Dickinson, D. F., Klein, M. J., Zimmermann, P. 1984. *Ap. J.* 283: 106
Kylafis, N. D., Norman, C. 1987. *Ap. J.* 323: 346
Lane, A. P. 1982. PhD thesis. Univ. Mass.
Lane, A. P., Johnston, K. J., Bowers, P. F., Spencer, J. H., Diamond, P. J. 1987. *Ap. J.* 323: 756
Lewis, B. M. 1989. *Ap. J.* 338: 234
Lewis, B. M., Engels, D. 1991. *MNRAS* 251: 391
Likkel, L., Morris, M. 1988. *Ap. J.* 329: 914
Likkel, L., Morris, M., Maddalena, R. J. 1991. *Astron. Astrophys.* In press
Liljestrom, T., Mattila, K., Toriseva, M., Anttila, R. 1989. *Astron. Astrophys. Suppl.* 79: 19
Litvak, M. M. 1970. *Phys. Rev.* A2: 2107
Litvak, M. M. 1974. *Annu. Rev. Astron. Astrophys.* 12: 97
Lockett, P., Elitzur, M. 1991. *Ap. J.* Submitted
Lucas, R., Cernicharo, J. 1989. *Astron. Astrophys.* 218: L20
Madden, S. C., Irvine, W. M., Matthews, H. E., Brown, R. D., Godfrey, P. D. 1986. *Ap. J.* 300: L79
Madden, S. C., Friberg, P., Brown, R. D., Godfrey, P. D. 1988. *IAU Circ. No.* 4537
Martin, J. M., Bottinelli, L., Dennefeld, M., Gouguenheim, L., Le Squeren, A. M. 1988. *Astron. Astrophys.* 201: L13
Martinez, A., Bujarrabal, V., Alcolea, J. 1988. *Astron. Astrophys. Suppl.* 74: 273
Martin-Pintado, J., Bachiller, R., Thum, C., Walmsley, M. 1989. *Astron. Astrophys.* 215: L13
Martin-Pintado, J., Thum, C., Bachiller, R. 1989. *Astron. Astrophys.* 222: L9
Mauersberger, R., Henkel, C., Wilson, T. L. 1987. *Astron. Astrophys.* 173: 352
McIntosh, G., Predmore, C. R. 1991. *Ap. J.* Submitted
McIntosh, G., Predmore, C. R., Moran, J. M., Greenhill, L. J., Rogers, A. E. E., Barvainis, R. 1989. *Ap. J.* 337: 934
Menten, K. M. 1991a. In *Skyline: Proc. 3rd Haystack Conf.*, ed. A. D. Haschick, P. T. P. Ho. Provo: Astron. Soc. Pac.
Menten, K. M. 1991b. *Ap. J. Lett.* In press
Menten, K. M., Melnick, G. J., Phillips, T. G. 1990a. *Ap. J. Lett.* 350: L41
Menten, K. M., Melnick, G. J., Phillips, T. G., Neufeld, D. A. 1990b. *Ap. J. Lett.* 363: L27
Menten, K. M., Reid, M. J., Moran, J. M., Wilson, T. L., Johnston, K. J., Batrla, W. 1988. *Ap. J. Lett.* 333: L83

Migenes, V., Cohen, R. J., Brebner, G. C. 1991. *MNRAS*. To be published
Mirabel, I. F., Rodriguez, L. F., Ruiz, A. 1989. *Ap. J.* 346: 180
Moore, T. J. T., Cohen, R. J., Mountain, C. M. 1988. *MNRAS* 231: 887
Moran, J. M., Greenhill, L. J., Reid, M. J. 1991. In *Frontiers of VLBI*, ed. H. Hirabayashi, M. Inoue, H. Kobayashi. Universal Acad.
Moran , J. M., Papadopoulis, G. D., Burke, B. F., Lo, K. Y., Schwartz, P. R., et al. 1973. *Ap. J.* 185: 535
Muchmore, D. O., Nuth, J. A., Stencel, R. E. 1987. *Ap. J. Lett.* 315: L146
Nedoluha, G. E., Watson, W. D. 1991. *Ap. J. Lett.* 367: L63
Neufeld, D. A., Melnick, G. J. 1990. *Ap. J. Lett.* 352: L9
Neufeld, D. A., Melnick, G. J. 1991. *Ap. J.* 368: 215
Norris, R. P., Booth, R. S. 1981. *MNRAS* 195: 213
Norris, R. P. 1985. *MNRAS* 216: 701
Nyman, L-Å, Olofsson, H. 1986. *Astron. Astrophys.* 158: 67
Nyman, L-Å, Johansson, L. E. B., Booth, R. S. 1986. *Astron. Astrophys.* 160: 352
Palma, A., Green, S., DeFrees, D. J., McLean, A. D. 1988. *Ap. J. Suppl.* 68: 287
Phillips, T. G., Kwan, J., Huggins, P. J. 1980. In *Interstellar Molecules*, ed. B. H. Andrew, p. 21. Dordrecht: Reidel
Plambeck, R. L., Wright, M. C. H., Carlstrom, J. E. 1990. *Ap. J. Lett.* 348: L65
Plambeck, R. L., Menten, K. M. 1990. *Ap. J.* 364: 555
Ponomarev, V. O., Strelnitskij, V. S., Chugail, N. N. 1990. *Astron. Tsirk.* 1545: 37
Reid, M. J. 1989. In *The Center of the Galaxy*, ed. M. Morris, p. 37. Dordrecht: Kluwer
Reid, M. J., Menten, K. M. 1990. *Ap. J. Lett.* 360: L51
Reid, M. J., Moran, J. M. 1981. *Annu. Rev. Astron. Astrophys.* 19: 231
Reid, M. J., Moran, J. M. 1988. In *Galactic and Extragalactic Radio Astronomy*, ed. G. L. Verschuur, K. I. Kellermann, ch. 6. New York: Springer. 2nd ed.
Reid, M. J., Silverstein, E. M. 1990. *Ap. J.* 361: 483
Reid, M. J., Haschick, A. D., Burke, B. F., Moran, J. M., Johnston, K. J., Swenson, G. W. 1980. *Ap. J.* 239: 89
Reid, M. J., Schneps, M. H., Moran, J. M., Gwinn, C. R., Genzel, R., et al. 1988. *Ap. J.* 330: 809
Rickard, L. J., Bania, T. M., Turner, B. E. 1982. *Ap. J.* 252: 147
Schmelz, J. T., Baan, W. A., Haschick, A. D. 1987. *Ap. J.* 321: 225
Schneps, M. H., Lane, A. P., Downes, D., Moran, J. M., Genzel, R., Reid, M. J. 1981. *Ap. J.* 249: 124
Spitzer, L. 1978. *Physical Processes in the Interstellar Medium* New York: Wiley
Stencel, R. E., Nuth, J. A., Little-Marenin, I. R., Little, S. J. 1990. *Ap. J. Lett.* 350: L45
Strelnitskij, V. S. 1980. In *Interstellar Molecules, IAU Symp. 87*, ed. B. H. Andrew, p. 591. Dordrecht: Reidel
Strelnitskij, V. S. 1984. *MNRAS* 207: 339
Szymczak, M. 1989. *MNRAS* 237: 561
Szymczak, M. 1990. *MNRAS* 243: 375
Tarter, J. C., Welch, W. J. 1986. *Ap. J.* 305: 467
te Lintel Hekkert, P., Habing, H., Caswell, J. L., Haynes, R. F., Norris, R. P. 1988. *Astron. Astrophys.* 202: L19
Troland, T. H., Heiles, C. 1986. *Ap. J.* 301: 339
Van Buren, D., MacLow, M.-M., Wood, D. O. S., Churchwell, E. 1990. *Ap. J.* 353: 570
Varshalovich, D. A., Kegel, W. K., Chandra, S. 1983. *Sov. Astron. Lett.* 9: 209
Walmsley, C. M. 1990. *Astron. Astrophys. Suppl.* 82: 201
Walmsley, C. M., Batrla, W., Matthews, H. E., Menten, K. M. 1988. *Astron. Astrophys.* 197: 271
Waters, J. W., Gustincic, J. J., Kakar, R. K., Kuiper, T. B. H., Roscoe, H. K., et al. 1980. *Ap. J.* 235: 57
Welch, W. J., Marr, J. 1987. *Ap. J. Lett.* 317: L21
Welch, W. J., Dreher, J. W., Jackson, J. M., Terebey, S., Vogel, S. N. 1987. *Science* 238: 1550
Wilson, T. L., Batrla, W., Pauls, T. A. 1982. *Astron. Astrophys.* 110: L20
Wilson, T. L., Walmsley, C. M., Snyder, L. E., Jewell, P. R. 1984. *Astron. Astrophys.* 134: L7
Wilson, T. L., Mauersberger, R., Brand, J., Gardner, F. F. 1987. *Astron. Astrophys.* 186: L5
Wilson, T. L., , Henkel, C. 1988. *Astron. Astrophys.* 206: L26
Wilson, T. L., Walmsley, C. M., Baudry, A. 1990. *Astron. Astrophys.* 231: 159
Wood, D. O. S., Churchwell, E. 1989. *Ap. J. Suppl.* 69: 831
Zell, P. J., Fix, J. D. 1991. *Ap. J.* 369: 506